Final Report

Nighttime Chemistry: Observations of NO_3 and N_2O_5

CARB 04-335

Principal Investigator

Ronald C. Cohen

Professor, Department of Chemistry and

Department of Earth and Planetary Science

University of California, Berkeley

Berkeley, CA 94720-1460

(510) 642-2735

(510) 643-2156 (FAX)

e-mail: rccohen@berkeley.edu

Report prepared for:

State of California Air Resources Board

Research Division

PO Box 2815

Sacramento, CA 95812

March 2008

Nighttime Chemistry: Observations of NO_3 and N_2O_5

Table of Contents **2**

Acknowledgements

The measurements described in this report were obtained by Chika Minejima and Paul Wooldridge and Ronald Cohen of UC Berkeley. We thank staff of ARB, John Karlik and Steve Murray for aid identifying and setting up a site for the measurements in the Central Valley and the staff at the UC Blodgett Forest Research Station for their assistance during our efforts at their site and Sierra Pacific Industries for generous permission to access to their land.

List of Figures

Executive Summary

An improved laser-induced fluorescence (LIF)technique for measurement of NO_3 and N_2O_5 was tested in the lab, packaged as a field instrument and deployed in 3 separate campaigns. Prior to this contract, the sensitivity of the improved instrument was projected to be in the range 10-25 ppt/min. During this contract we demonstrated sensitivity of ±25 ppt/min. We developed methods for measuring zero that permit long averaging and result in an uncertainty of less than ±1ppt in the instrument zero for averages over several hours. The detection uncertainty was shown to scale as the square root of time and to be ±3 ppt for 1 hour and ±1 ppt for 5 hour averages. Measurements obtained during the research described in this report, show that the technique used here is suitable for measurements in the surface layer (~0-20 m) as well as in the nocturnal (~20-120 m) and residual layers (~120-1000 m) above. The higher concentrations expected aloft would be much easier to measure than those observed during this study.

This new instrument was used to make observations of the sum of NO_3+N_2O_5 and of NO_3 were made at the University of California, Blodgett Forest Research Station (UC-BFRS 38° 54′ 45″ N, 120° 39′ 27″ W, 1315 m ASL) during August and September 2006 and November and December 2006 and at an orchard just outside the town of Arvin in the southern end of the San Joaquin valley (35° 12' 31" N, 118° 46' 33" W, 617 m ASL) during March 2007. In the two UC-BFRS deployments mixing ratios of the sum of NO_3+N_2O_5 averaged 4±1 ppt and measurements of NO_3 were below the detection limit of 1ppt. Calculations indicate the N_2O_5/NO_3 ratio at this site was in the range 0.8-1.4 in summer and 2-12 in winter. Mixing ratios of both NO_2 which is the source of NO_3 and N_2O_5 and of the sum of NO_3+N_2O_5 were much larger at the Arvin site, where NO_3+N_2O_5 ranged as high as 300 ppt and averaged 25 ppt at night.

The chemical production rate and partitioning of NO_3 and N_2O_5 are well known. Thus the measured concentrations provide information about transport and removal processes. The measurements indicate that essentially all of the NO_3 and N_2O_5 produced in the surface layer are removed before sunrise. Analysis of these results establishes that the process that destroys the sum of NO_3+N_2O_5 in the surface layer at night had a time constant of less than 10 minutes at the times and locations of our measurements. We find that VOC reactions of NO_3 were most often the primary sink of N_2O_5 + NO_3.

This conclusions is consistent with other recent field campaigns that were able to sample different parts (or in same cases all 3 components) of the lowest regions of the nocturnal atmosphere--the surface, nocturnal and residual layers. All of these recent studies indicate that the sum of NO_3+N_2O_5 has a very short lifetime within the surface layer, and that the lifetime grows longer in nocturnal boundary layer and longer still in the residual layer above that. Because of the bigger lifetime aloft, processes occurring above the surface layer will be the ones that have a variable effect on the extent to which NO_x that is converted to NO_3 and N_2O_5 is available for reconversion back to NO_x of the end of the night. Also, in the slower chemical environment present aloft, there is more potential for varying the relative importance of

different reaction pathways for removal of NO_3 and N_2O_5 and thus experiments in these regions could more clearly test current models of aerosol reactions.

The observations and analysis presented here supports a growing body of research that identifies the removal mechanism for NO_3 and N_2O_5 as one of the key uncertainties in models of O_3 and PM. In particular, the fate of the products of NO_3 + VOC reactions remain poorly understood. We do not know whether the predominant products are NO_2, HNO_3, or one of the many possible $RONO_2$ species. We do not know the extent to which these $RONO_2$ are incorporated into SOA.

Disclaimer

The statements and conclusions in this report are those of the authors from the University of California and not necessarily those of the California Air Resources Board. The mention of commercial products, their source, or their use in connection with the material reported herein is not to be construed as actual or implied endorsement of such products.

Nighttime Chemistry: Observations of NO_3 and N_2O_5

1. Introduction

Emissions and secondary production of NO_x from stationary and mobile sources of combustion and from application of fertilizers are widespread in California. NO_x is eventually removed from the atmosphere by deposition primarily in the form of HNO_3, or hydroxy organic nitrates. Prior to removal, however, nitrogen oxides contribute to the production of ozone and aerosol. One of the major outstanding questions regarding the chemistry and transport of NO_x is the assessment of what happens at night [Stutz et al. 2004; Wood et al., 2005, Brown et al., 2006, Sommariva et al., 2007]. While the photochemical and transport lifetimes of NO_x are about 4 daytime hours in the summer, evidence shows that there is still a build up of NO_x over urban areas that reflects accumulation over several days, implying that nighttime chemistry is not fully removing the NO_x that remained in the atmosphere at sunset and that this NO_x contributes to production of O_3 on the subsequent days [e.g. Murphy et al., 2006a,b]. There is also evidence that nighttime NO_x chemistry depletes the O_x reservoir in urban regions in California and elsewhere [Murphy et al., 2006b and Brown et al., 2003a, 2004, 2006]. The connection between nighttime NO_x chemistry and inorganic nitrate aerosol or secondary organic aerosol (SOA) is more tenuous. Laboratory measurements and model calculations support the idea that NO_3 and N_2O_5 chemistry can be an important source of both types of aerosol but field measurements to test the elements of these ideas either qualitatively or quantitatively do not yet exist. Nonetheless, there is a growing body of evidence suggesting oxidation of anthropogenic and biogenic alkenes by NO_3 are an important source of SOA.

The nighttime chemistry associated with production of NO_3 and N_2O_5 and subsequent reactions of these molecules with VOC and aerosol have been studied extensively in the lab. However, field observations and models are not yet well developed. Until recently, field observations have been limited because of the difficulty of detecting NO_3 and N_2O_5 [Simpson et al., 2003; Wood et al., 2005, Brown et al., 2006], except over long path lengths using absorption spectroscopy. Modeling studies have paid relatively little attention to the subject because of the difficulty of adequately representing nocturnal layers and their mixing, because of the belief that nocturnal chemistry is not particularly important to production of ozone or particulate matter and because the observations were not available to provide rigorous tests of the chemistry.

Initial steps in the nighttime chemistry of NO_x—the rates of the reactions of NO_2 with O_3, of NO_3 with NO_2 and the decomposition rate of N_2O_5—are well established based on laboratory measurements [Sander et al., 2006]. Recent field measurements described by Brown et al. [Brown et al., 2003b] confirm the lab results for the equilibrium constant for the reaction of NO_2 with NO_3 to produce N_2O_5 are consistent with atmospheric observations. Also, the chemistry that results in conversion of NO_3 or N_2O_5 back to NO_x (reaction of NO_3 with NO and photolysis of both species) is well known. Despite this knowledge, we are unable to accurately calculate the amount of NO_x that is permanently removed from the available pool by nighttime chemistry because of considerable uncertainties in the description of the nocturnal boundary layer [e.g. Geyer, 2004; Stutz, 2004] and because the chemistry of NO_3 and N_2O_5 involving 1) NO_3 reactions with VOC in the gas and aerosol phase, 2) N_2O_5 reactions in the gas and aerosol phase and 3) rates of deposition to surfaces are poorly understood. Most importantly, there are few observations available to test the quality of current thinking about NO_3 and N_2O_5.

The principle objectives of the project supported by this contract were 1) to complete the development of an improved laser-induced fluorescence technique for measurement of NO_3 and of N_2O_5 by thermal dissociation to produce NO_3 and 2) to demonstrate the capabilities of our improved LIF approach in the field. Secondary objectives were 1) to provide a baseline of observations of NO_3 and N_2O_5 at a (preferably urban) site in the central valley that is strongly affected by NH_4NO_3 aerosol and at a rural site (UC Blodgett Forest), and 2) to advance our understanding of the processes by which and extent to which nighttime chemistry involving NO_3 or N_2O_5 serves to remove NO_x and O_3 from the atmosphere while simultaneously producing NO_2, HNO_3 and/or organic nitrates. In Section 2 of this report we provide additional background. In Section 3 we describe the instrument development and evaluation and in Section 4 we describe the measurement sites and observations. In Section 5 we present analysis and discussion of the observations. Finally the report concludes and makes recommendations for future research in Section 6.

2. Background

The nitrate radical (NO_3) and dinitrogen pentoxide (N_2O_5) are uniquely important to the nocturnal chemistry of the troposphere. NO_3 is produced by the reaction of nitrogen dioxide (NO_2) with ozone (O_3):

$$NO_2 + O_3 \xrightarrow{k_1} NO_3 + O_2 \qquad (1)$$

Reaction 1 is slow: at 3°C (278 K), k_1 is equal to 1.8×10^{-17} cm^3 $molecule^{-1}$ s^{-1}, resulting in a lifetime for NO_2 at 60 ppbv of O_3 of 12 hours. This is the lowest temperature relevant to our study. At higher temperatures the NO_2 lifetime is shorter. Equilibrium is established between NO_2, NO_3, and N_2O_5 on timescales of a few minutes:

$$NO_2 + NO_3 + M \longleftrightarrow N_2O_5 + M \qquad (2)$$

This equilibrium is strongly shifted to the right at low temperature. For example, at 3º C and 5 ppbv of NO_2, the $[N_2O_5]$:$[NO_3]$ ratio is 80. The rapid removal of a second NO_2 molecule upon formation of N_2O_5 reduces the effective lifetime of NO_2 at 60 ppb O_3 by a factor of 2. Thus even at the lowest temperatures where the chemistry is slow in 12 hours of darkness 90% of NO_2 is converted to NO_3 or N_2O_5. The NO_2 lifetime in summer is short, with most NO_2 present at sunset being converted to NO_3 and N_2O_5 prior to sunrise, as long as O_3 is present in large excess. The equilibrium between NO_3 and N_2O_5 shifts toward NO_3 at warmer temperatures.

If the N_2O_5 and NO_3 are not rapidly converted to more stable NO_y species (e.g. HNO_3, aerosol NO_3^-, organic nitrates), then they are returned to the active pool of NO_x upon sunrise as a result of the rapid photolysis of NO_3 (overhead photolysis rate ≈ 0.2 s^{-1}), reaction of NO_3 with NO and the thermal decomposition of N_2O_5. In the boundary layer, it is assumed that the typical situation is that a large fraction N_2O_5 and NO_3 are removed over the course of the night. This nocturnal chemistry affects the concentrations of volatile organic compounds (VOCs) and NO_x ($NO_x \equiv NO + NO_2$) and O_x ($O_x \equiv O_3 + NO_2$). NO_3 reacts rapidly with alkenes and calculations suggest that it is the predominant oxidant for some biogenic VOCs. N_2O_5 hydrolyzes on surfaces to form nitric acid (HNO_3) [R3], and this reaction is thought to be important for removal of NO_x from the global troposphere and under conditions of high aerosol loading locally within the planetary boundary layer:

$$N_2O_5 + H_2O_{(l)} \xrightarrow{heterogeneous} 2HNO_3 \quad (3)$$

Laboratory and smog chamber measurements of the uptake coefficient (γ) for this heterogeneous reaction varies from 0.02 for uptake onto $NaNO_3$ aerosol at 90% RH [Wahner, et al. 1998] to over 0.1 for uptake onto pure H_2SO_4/H_2O aerosol [Hanson, 1997; Robinson, 1997]. The uptake coefficient represents the efficiency of reaction upon collision of a gas molecule with a surface, with a γ=1 representing reaction on every collision and γ=0.01 reaction on only 1 in every 100 collisions. Typical models of boundary layer aerosol use a γ of 0.02-0.06 [e.g. Evans et al., 2005; Liao et al., 2005]. However, Brown et al. have shown that the γ for ambient aerosol is lower and that the γ varies by an order of magnitude with higher rates for more sulfate rich aerosols, γ=0.017±0.004 (corresponding to reaction on 1 in 50 collisions), than for more ammonium rich. γ=<0.0016, aerosol (corresponding to reaction on less than 1 in every 500 collisions) [Brown et al. 2006].

Prior to 2000, atmospheric N_2O_5 had only been measured by long-path absorption spectroscopy in the stratosphere [e.g. Zhou, 1997; Sen, 1998], and NO_3 had only been measured by Differential Optical Absorbance Spectrometry (DOAS) [Platt, 1994; Heintz, 1996] and Matrix Isolation – Electron Spin Resonance Spectrometry (MI-ESR) [Geyer, 1999]. DOAS techniques sample across a long path-length over which it is difficult to demonstrate that concentrations of NO_3, N_2O_5, and their sources (NO_2 and O_3) and sinks (VOC and aerosol) are uniformly distributed making it desirable to have an *in situ* measurement capable of point sampling for testing chemical models. MI-ESR is one such method, but it is too difficult and time consuming for widespread application. In the last 5 years, several new approaches have been developed. We described a laser-induced fluorescence approach to NO_3 detection with detection of N_2O_5 by thermal dissociation followed by NO_3 detection [Wood et al., 2003, 2005]. We demonstrated detection of NO_3 and N_2O_5 with 76 ppt/min sensitivity under field conditions [Wood et al., 2003, 2005]. Matsumoto et al. applied the LIF technique to NO_3 and N_2O_5 reporting a sensitivity to NO_3 of 32 ppt/min [Matsumoto et al., 2006]. Instruments using Cavity Ring Down Spectroscopy (CRDS) and its variations including Cavity Enhanced Absorption Spectroscopy (CEAS) have been described with rapid time response (0.04-0.2 Hz) and high sensitivity to NO_3 (0.1-2 ppt/min) [Brown et al., 2002a,b, 2003a; Simpson, 2003; Ball et al., 2004; Ayers et al., 2005; Bitter et al., 2005; Dubé et al., 2006; Venables et al., 2006]. Many of these instruments measure N_2O_5 following thermal dissociation with detection of NO_3. Another new approach developed is based on chemical ionization mass spectrometry (CIMS). [Slusher et al., 2004] to measure the sum of NO_3 and N_2O_5 by reactions with I^- yielding NO_3^- with a detection limit of about 2 ppt/min but only at extremely low humidity present at the surface in Antarctica or in the upper troposphere. An intercomparison of most of these techniques was performed in June 2007 at the SAPHIR chamber in Juelich, Germany. Final data has not yet been released and detailed analyses are still in progress, but the preliminary data available at the time of this writing suggest overall good agreement among multiple different implementations of 3 fundamentally distinct detection methods.

NO_3 mixing ratios of up to a few hundred ppt have been observed in urban plumes [Wayne, 1991] and mixing ratios up to 40 pptv are common in more remote regions [Wayne, 1991; Carslaw, 1997; Geyer, 2001; Brown, 2003a; Simpson, 2003]. N_2O_5 mixing ratios of up to 3 ppbv have been observed near Boulder, Colorado [Brown, 2003a]. In northern latitudes and in the marine boundary layer N_2O_5 mixing ratios of less than 100 pptv are more common [Simpson, 2003; Brown, 2004]. It is often useful to express the fraction of nighttime NO_x

reservoirs (NO_3 + 2 x N_2O_5 + NO_2) that are present as NO_3 +2x N_2O_5. Fractions as high as 40 % have been routinely observed (Figure 1 (b) and (c)).

Measurements in a variety of locations have indicated that the NO_2 removed at night by reaction 3 can be comparable in magnitude to the loss of NO_2 during the day by reaction with OH [Heintz, 1996; Martinez, 2000; Wood, 2005]. To date, there have been no systematic studies of the nitrogen oxide budget at night that included both measurements of NO_3 and N_2O_5 and of their reaction products HNO_3 and organic nitrates.

Recent modeling of the vertical profiles expected for NO_3 and N_2O_5 under a range of conditions [Geyer et al., 2004; Stutz et al., 2004] and measurements of vertical profiles by Brown et al. have sharpened our community's focus on the structures expected in vertical profiles of NO_3 and N_2O_5. Brown et al. [2007], show that it is useful to think of the layered structure of the atmosphere at night as having three weakly communicating compartments: a surface layer, a nocturnal boundary layer and a residual layer. These layers grow and shrink during the night and the divisions between them are marked by inflections in potential temperature as shown in Figure 1 (a), reproduced from Brown et al. 2007. These layers have distinctly different O_3, NO_2 and temperature (Figure 1 (b and c)) resulting in different source strengths for NO_3 and N_2O_5. The layers also exhibit different lifetimes for N_2O_5 and for NO_3 reflecting the vertical variation of VOC, of aerosol sinks and of NO.

In light of these and other recent findings, the main reasons for interest in the chemistry of NO_3 and N_2O_5 are 1) understand how much NO_x remains in the atmosphere after a night of chemical processing, 2) to understand whether higher oxides such as organic nitrates and HNO_3 that are produced during removal of NO_3 and N_2O_5 have important consequences for the chemical production of O_3 or PM and 3) to understand how this chemistry affects the spatial and temporal patterns of nitrogen deposition. To advance our understanding of these issues, questions that we must address about mechanistic chemistry of the nighttime NO_x reservoirs (NO_3 and N_2O_5) are ones regarding the source of these species and their partitioning and ones regarding their sinks:

1) Is the rate production of NO_3 and its equilibrium with N_2O_5, as it occurs in the atmosphere, consistent with laboratory measurements of the formation rate of NO_3 and of the equilibrium constant for the reaction of NO_3 with NO_2 to form N_2O_5?

2) At what rate and by what processes are these nighttime species removed from the atmosphere or converted to species that are chemically stable during the daytime?

2a) To what extent is the removal of NO_3 and N_2O_5 due to reactions of NO_3 with VOC or of N_2O_5 on the surfaces of aerosol?

2b) What are the nitrogen containing products of the reactions of NO_3 with VOC? NO_2? HNO_3? Organic nitrates? Do they partition into aerosol immediately or upon subsequent oxidation?

The component of question 1 about the partitioning of NO_3 and N_2O_5 has been largely laid to rest by the recent measurements of Brown et al. [2003]. In these series of field experiments the rate constants for the N_2O_5 equilibrium have been shown to accurately describe atmospheric measurements. The source reaction (R1) of NO_2 with O_3 is thought to be accurate to better than 20%. Thus models that accurately represent O_3 and NO_2 will accurately represent the sources and partitioning of NO_3 and N_2O_5. As an aside, we note that the network of "NO_2" measurements does not measure NO_2 but something more like NO_y and so model calculations

of NO_2 cannot be validated by direct comparison to the measurement network [Winer et al., 1974; Dunlea et al., 2007; Steinbacher et al., 2007].

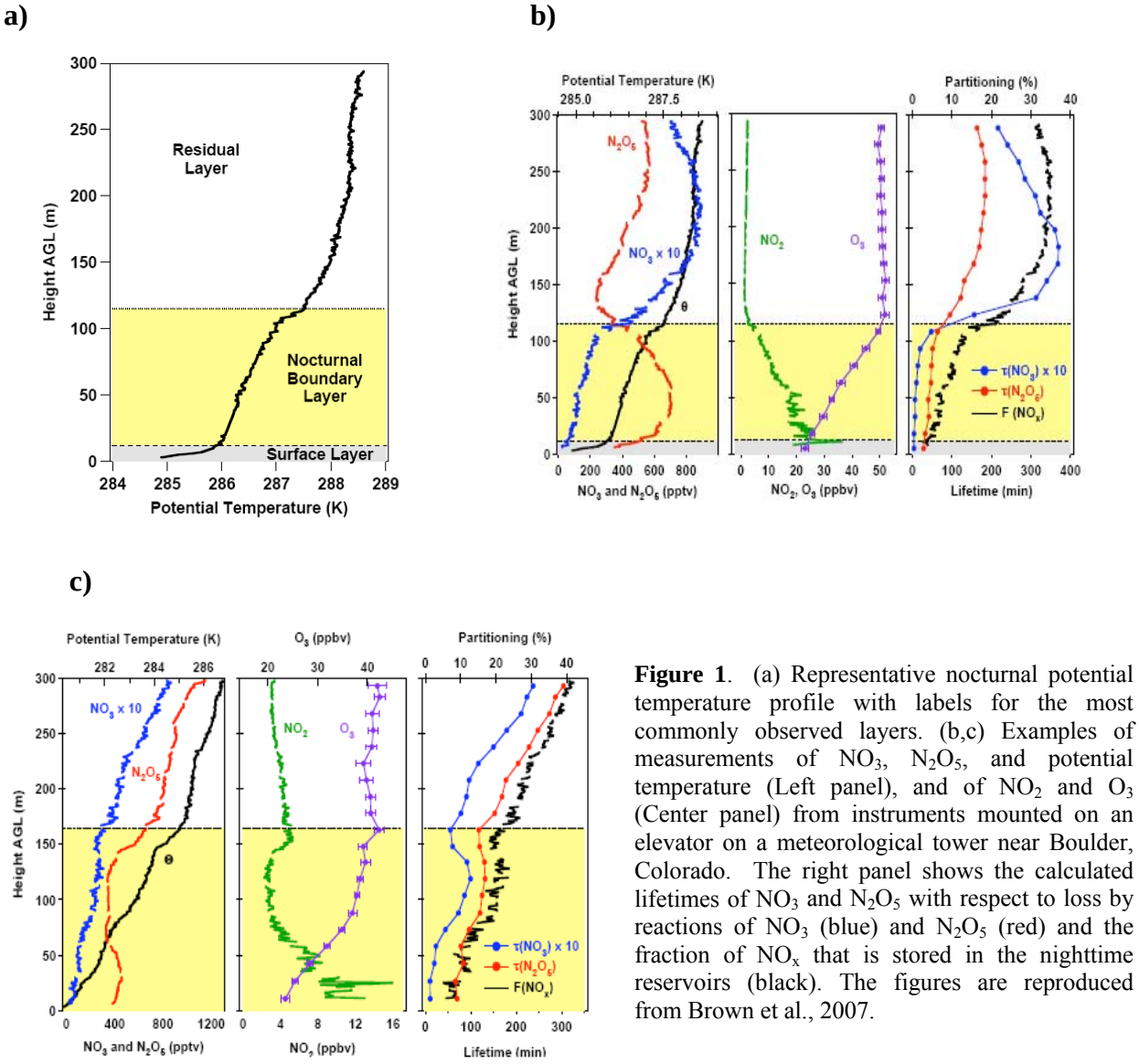

Figure 1. (a) Representative nocturnal potential temperature profile with labels for the most commonly observed layers. (b,c) Examples of measurements of NO_3, N_2O_5, and potential temperature (Left panel), and of NO_2 and O_3 (Center panel) from instruments mounted on an elevator on a meteorological tower near Boulder, Colorado. The right panel shows the calculated lifetimes of NO_3 and N_2O_5 with respect to loss by reactions of NO_3 (blue) and N_2O_5 (red) and the fraction of NO_x that is stored in the nighttime reservoirs (black). The figures are reproduced from Brown et al., 2007.

Question 2 about the sinks of NO_3 and N_2O_5 has not been adequately addressed by previous observations. Recent observations by Brown et al.[2007], Murphy et al.[2006a,b], and Geyer et al.[2001] have clarified a now framework for addressing some of the key questions. This field research coupled to our understanding from laboratory measurements shows that there are two branches removing the nocturnal nitrogen oxides. The first is reaction of NO_3 with anthropogenic and biogenic alkenes and aldehydes. There are other NO_3 reactions that can have important secondary effects such as the reactions of NO_3 with peroxy radicals [e.g. Biggs et al., 1994, 1995; Stockwell et al., 1997; Vaughan et al., 2006] but these are not directly important to the concentration of NO_3 or N_2O_5. The second is the reaction of N_2O_5 on aerosol. The observations by Brown et al.[2006] have shown that the chemical composition of aerosol matters and that the rate for this reaction varies with aerosol composition by at least an order of

magnitude as noted above [Brown et al. 2006]. These initial observations by Brown et al. provide examples of the possible range but they do not provide sufficient data upon which to generalize to the full variety of aerosol chemical composition observed in the atmosphere. Only simultaneous measurements of aerosol composition, NO_3 and N_2O_5 in many locations that have a variety of aerosol types will provide the data needed to guide development of mechanisms that represent this aerosol composition effect. Of course, these locations need to be ones where the aerosol loss term is important.

In addition to field observations for evaluating these two classes of chemical processes, even more important from the point of view of modeling NO_3 and N_2O_5 is the fact that there is strong layering during the night and what matters for the overall lifetime of NO_x is not the processing that occurs at any single height but the integral over the full depth of the surface, nocturnal and residual layers (Figure 1). Measurements of NO_3 and N_2O_5 and other nitrogen oxides at a single height are appropriate for testing mechanisms. Once these mechanisms are established with more confidence, evaluating their implementation in regional air quality models will require evaluation of the nocturnal layering in the model along with the model representation of the reactivity of VOC to NO_3 and aerosol to N_2O_5 in those layers. The signals for NO_3 and N_2O_5 are higher within the nocturnal and residual layers as shown by the measurements of Brown et al. [2007].

Stutz et al.[2004] have pointed out that one factor driving low NO_3 in the nocturnal layer is NO emissions and described many of the basic features that would be expected if the atmosphere behaved as a single column model. Many of the features reported by Brown et al.[2007] bear some similarity to these model calculations. However, we also note that emissions are quite heterogeneous in space and there has not yet been adequate theoretical attention to the atmospheric variation expected if instead of a continuous source one is sampling air that passes over a locally strong source (e.g. a highway) and then proceeds to flow through a region of low or zero NO emissions.

In summary, we believe the chemistry of NO_3 and N_2O_5 is an important determinant of O_3 and likely also of particulate matter formation. However the accuracy and completeness of the chemistry and meteorology describing these processes in air quality models has not been adequately tested with field observations. While the chemical sources of NO_3 and N_2O_5 are well known, their sinks are not. The key unknowns for evaluating model performance are a) the rate of removal of NO_3 and N_2O_5 by chemical sinks, the identity of the products formed and the chemical lifetime of those products, b) the structure of the lowest atmospheric layers at night and the extent to which air in these layers is incorporated into the growing well-mixed daytime boundary layer on the following day. A deeper understanding of these issues is essential for complete analyses of atmospheric phenomenon that have an important role in regulatory policy—notably the weekend effect in NO_x, O_3 and particulate matter and the extent to which poor air quality on one day is likely to lead to a problem that will persist for multiple days.

3. A pulsed diode laser approach to LIF detection of NO_3

3.1 Design goals

The LIF technique we described in Wood et al. [2003] is much less sensitive than CRDS and its variants, however, LIF has the advantage that there is much less contact of the sample with the

walls and it should be possible to configure an LIF instrument such that it is insensitive to aerosol without inserting a particle filter into the sampling lines. Particle filters used for CRDS by Dubé et al. [2006] and other CRDS groups require frequent changes and are not suitable for use in long term monitoring. Use of a diode laser for excitation in our LIF instrument also greatly reduces the cost relative to the cost of the initial CRDS instruments that use a high power dye laser. However, recently CRDS instruments have been developed (although not yet described in the literature) using these same diodes, so low cost is no longer a unique advantage of LIF.

The photophysics of NO_3 relevant to LIF detection are discussed in detail in Wood et al. [2003, 2005]. Briefly, NO_3 has a strong absorption at 662 nm and a long fluorescence lifetime, similar to the fluorescence lifetime of NO_2. However, the fluorescence quantum yield is much lower than expected based on scaling of parameters relative to NO_2. This implies extremely strong conversion of the excitation to a non-fluorescing (dark) state. Still the fluorescence is strong enough that reasonable sensitivity can be achieved for an LIF experiment. Wood et al. achieved 76ppt/min at S/N = 2 using a continuous diode laser system. As described below, we projected sensitivity of at least 25 ppt/min could be achieved using a pulsed diode laser with time gated detection. Pulsed excitation and time gated detection has the additional advantage of reducing the effects of aerosol scattering on the instrument background, eliminating one of the problems with LIF identified in the field trial of Wood et al. [2005].

The design strategy we developed requires diode lasers with both 50-200 mW output (under continuous operation) at 662.9 nm and sufficiently high beam quality (low divergence and circular output) to couple to a multi-pass cell. We proposed to create 100 ns pulses with 100 ns laser off periods from these diodes to achieve roughly 50% duty cycle for excitation. The design goal was to then detect fluorescence signal for 75 ns after an approximately a 25 ns delay from the end of the laser pulse. Since the fluorescence lifetime of NO_3 is 0.5 μs at 2 Torr, the detection of NO_3 fluorescence was calculated to be reduced by only slightly more than the duty cycle and to about 1/3 of the cw value. Combining the excitation duty cycle of 1/2 and the detection duty cycle of 1/3 results in an overall signal that was calculated to be 1/6 of that possible with a continuous laser source. Assuming a 100 mW laser and a 40 pass multi-pass cell we projected signal rates of order 100 counts-s^{-1}-ppb NO_3^{-1}. The main advantage of this strategy over the design we previously employed is the tremendous reduction in the laser-induced background, especially that due to prompt scattering of aerosols. The laser induced background count was projected to be reduced by a factor of 1000 to 3 counts-s^{-1} and the thermal background counts from the PMT is projected to be reduced by 2/3 to about 8 counts-s^{-1}. The sensitivity was projected to be in the range of 10-25 ppt-min^{-1} depending on whether the different design criteria could all be implemented simultaneously.

3.2 Optimized optical configuration

During the initial months of this contract we tested electrical circuitry for pulsing diode lasers, optical filters for rejecting laser scatter and optimized fluorescence collection. We tested a variety of combinations of laser pulse widths, and delays and gate widths for the fluorescence detection. The design we settled on after these tests is as follows (Figure 2). Light from a pulsed multi-mode 662 nm InAlGaP laser diode enters a 38-pass White cell perpendicular to the gas flow and induces excitation in the $\widetilde{B}\,^2E'(0000) \leftarrow X^2A'_2(0000)$ band of NO_3. The bandwidth of the 662 nm laser is 0.3 nm, which is much smaller than 4 nm wide (FWHM) NO_3 peak and is coarsely tuned by adjustment of the diode temperature and current. Its duty cycle is 50 % with

100 ns on and 100 ns off. The continuously operating diode power is 60 mW and the average power in pulsed mode is 30 mW. Fluorescence is measured orthogonal to the gas flow and laser axes. Approximately 4 % of the fluorescence is collected and collimated by a 51 mm – focal length lens mounted above the laser beam. A concave mirror (40 mm radius of curvature) sits

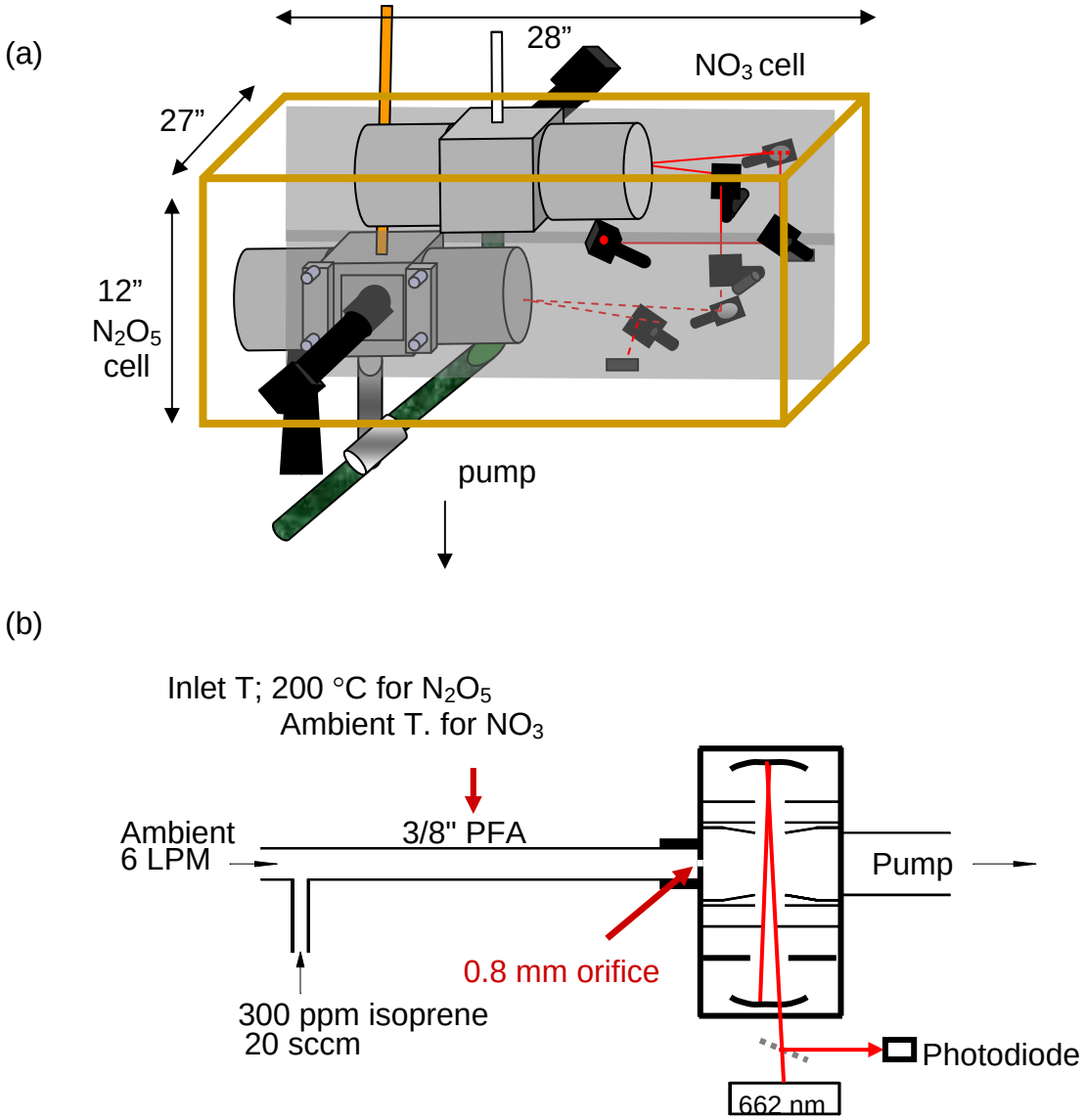

Figure 2. a) layout of 2 detection cells. The laser is located near the center of the optical plate. Sampling is from inlets that are perpendicular to the plane of the laser beamInlet geometry and flows of sample (6 LPM) and zeroing gas (300ppm isoprene at 20 sccm).

below the laser beam and increases the fluorescence signal by 80 %. The fluorescence then sequentially passes through two 700 nm long-pass filters and is then focused onto the photocathode of a thermoelectrically cooled GaAs photomultiplier tube (Hamamatsu H7421-50) equipped with an internal preamplifier and discriminator. Pulses from the PMT are counted by a multi-function data acquisition board. These filters transmit more than three quarters of the total NO_3 fluorescence [Nelson et al., 1983; Kim et al., 1992] while greatly reducing nonresonant

background. Laser scatter and light leaks (e.g., solar scatter) are minimized by use of highly reflective mirrors, by geometric baffling of stray light, and by coating the interior of the detection cell with a black optical paint. Thirty-eight passes in the White Cell was found to be a good balance between the favorable increase in laser fluence in the detection cell and the unfavorable increase in scattered light.

For a successful implementation of a pulsed detection scheme the diode laser must be fully off during the "off cycle." Evaluating the quality of the off state, was the first step in demonstrating that the elements of our improved approach would work. As part of the design optimization, we tested two different laser systems. Laser diodes assembled in our lab with custom electronics performed slightly better than a commercially available pulsed laser diode because of higher laser powers and shorter tails after the pulses. However, these were not stable enough in the face of environmental changes in temperature and humidity to use reliably in the field. We opted to use the turn key laser (Power Technology Inc, Model IQ1H80 (658-90) G3-R4) which is more stable but the laser pulse shuts off more slowly. As a result, achieving a fully off condition for the laser required a longer delay (60 ns vs. 25 ns) than we initially estimated resulting in a shorter time for an open gate during the off condition and corresponding decrease in signal rate by almost a factor of 2 (to 1/10 of the cw value). Based on the ratio of pressure dependent scattering (assumed to all be Raman scattering of O_2 and N_2) during the laser on period and during the gate set within the off cycle, the laser power in the off state is 0.006 of the power during the on cycle (166 times lower). As a result, there remain small contributions to the signal from N_2 and O_2 Raman and aerosol scatter. We tested a wide range of gate widths and found the optimum was a 40 ns wide detection gate.

Calculations suggest that the signal rate should be insensitive to pressure so long as we keep the pressure below 5 Torr as below this pressure the NO_3 fluorescence lifetime remains long compared to the gates ~200ns. We calculate that about 23% of the signal falls within the gates, 17% in the first gate, 5% in the second and 2% in the third. Observations in our lab are consistent with this overall estimate.

This pulsed laser system has typical signal rate of 36 cps/ppb NO_3 and a background of approximately 20 counts/s. The scatter is about twice our optimistic expectations of 11 counts/s. The overall instrument sensitivity at S/N = 2 is approximately 25 ppt-min^{-1} within the range promised in our proposal. This is a factor of three improvement over the CW experiment that had been field tested prior to this project. There is still room for improvement in the design and we are hopeful that future improvements that reduce the power when the laser is off, decrease the scatter using a new optical black coating that we have recently identified, and increase the laser power available using either dye or diode lasers will bring the sensitivity to below 5ppt-min^{-1}.

At the signal rate of 36 cps/ppbNO_3 one count is equal to 30 ppt. Thus temporal stability of the background is as important as modest improvements in S/N. The background signal consists of two parts: 1) signal from the detector in the absence of NO_3 or any other molecular absorbers; and 2) the fluorescence from other chemical species, of which the only important term is NO_2. We measured the NO_2 fluorescence rate at 662 nm to be 0.08 counts/s/ppb. We measured the background due to both these terms for 30 seconds every 30 seconds. At different times, we measured the instrument background due to both of these terms by 1) flowing zero air into the inlet, 2) by adding NO, which reacts with NO_3 converting it to NO_2, 3) by adding isoprene, which reacts with NO_3 converting it to NO_2, $RONO_2$, or 4) by pulling the air through a long coil of tubing to react away N_2O_5 and NO_3. Both the zero air and the coil approach removed a

large fraction of aerosols and contributed to a slight decrease in the background (at the level of a fraction of a count). We also found a small positive artifact (1-2 counts/s) from addition of NO and so ultimately chose addition of isoprene as the most accurate method of zeroing. We demonstrated that the zero can be averaged over half hour periods when the instrument is thermally stable and is accurate to 0.1 counts corresponding to a zero uncertainty of no more than 3 ppt. Nonetheless, we note that because both the signal and the zero are quantities that have noise on them, the difference between them can be negative and still represent a statistically valid measurement.

3.3 Calibration and sampling

NO_3 and N_2O_5 react rapidly on surfaces. We use ¼ OD PFA Teflon tubing for the inlets and keep them as short as possible (~10 cm) with flows of 1-2 standard liters a minute to keep the residence time sufficiently short so that there are not significant surface losses.

The instrument was calibrated using procedures described in Wood et al. [2003]. NO_3 produced by the thermal dissociation of N_2O_5 is introduced into the fluorescence cell.

$$N_2O_5 + M + \text{heat} \rightarrow NO_2 + NO_3 + M \qquad (1)$$

The N_2O_5 is produced by mixing gaseous NO_2 and O_3 with NO_2 in stoichiometric excess using a small reaction vessel and several hour long reaction time:

$$NO_2 + O_3 \rightarrow NO_3 + O_2 \qquad (2)$$

$$NO_2 + O_3 + M \rightarrow N_2O_5 + M \qquad (3)$$

Ozone is produced by photolysis of zero air at 185 nm using a mercury lamp and quantified using the 254 nm line of a second mercury lamp. Typically, 14 ppm of N_2O_5 is synthesized and diluted to 50~500 ppb. This N_2O_5 was either used directly as a mixture high in NO_2 or alternatively N_2O_5 was synthesized, crystallized and stored at low temperature with impurities removed by vacuum.

The mixing ratio of NO_3 is measured by converting it to NO_2 by reaction with NO. A flow of NO in N_2 (Praxair) is injected into the end of the flow tube. Reaction with NO rapidly converts the NO_3 into NO_2.

$$NO + NO_3 \rightarrow NO_2 + NO_2 \qquad (4)$$

Adding NO at the end of the inlet heating tube enables us to take the NO_3 wall loss into calibration. As the N_2O_5 was prepared with NO_2 in excess, complications arising from the much slower reaction $NO + O_3$ are minimal. Light from either 532 nm or 408 nm was used to detect NO_2. NO_3 does not contribute to the fluorescence used to quantify the NO_2 as both wavelengths are short enough to result in complete dissociation of NO_3.

Two steps are required to obtain each point on the NO_3 calibration curve:

(step 1) After measuring the background NO_2, N_2O_5 is thermally dissociated in the flow tube, producing a mixture of NO_2 and NO_3 in the detection cell. The 662 nm laser light is directed into the detection cell and the NO_3 fluorescence is measured. Then, the 532/408 nm laser light is directed into the detection cell and the NO_2 fluorescence is measured.

(step 2) NO is added to the $NO_2 + NO_3$ mixture at the end of the flow tube. This rapidly converts the NO_3 into NO_2. NO_3 and NO_2 are measured as above.

The NO_3 mixing ratio is calculated in step 2 as half the difference in NO_2 mixing ratio with and without added NO:

$$[NO_3]=0.5*\{[NO_2]_{(step\ 2)} - [NO_2]_{(step\ 1)}\} \quad (5)$$

The factor of 0.5 accounts for the stoichiometry of reaction 4. As a check, this number should be equal to the increase in NO_2 observed in Step 1 and equal to the NO consumed. Figure 3 shows an example of the calibration using NO. We also note that subsequent to the completion of this contract the instrument was compared with several other instruments using independent techniques at the large environmental chamber, SAPHIR, in Juelich, Germany. Detailed analysis of the comparison data is ongoing, but the general result indicates the calibration is accurate to at least 20% (possibly better). Calibration of the instrument was repeated in the laboratory immediately before and after each campaign. Measurements of the instrument sensitivity to Raman scattering was measured on a daily basis to track any changes of the laser alignment.

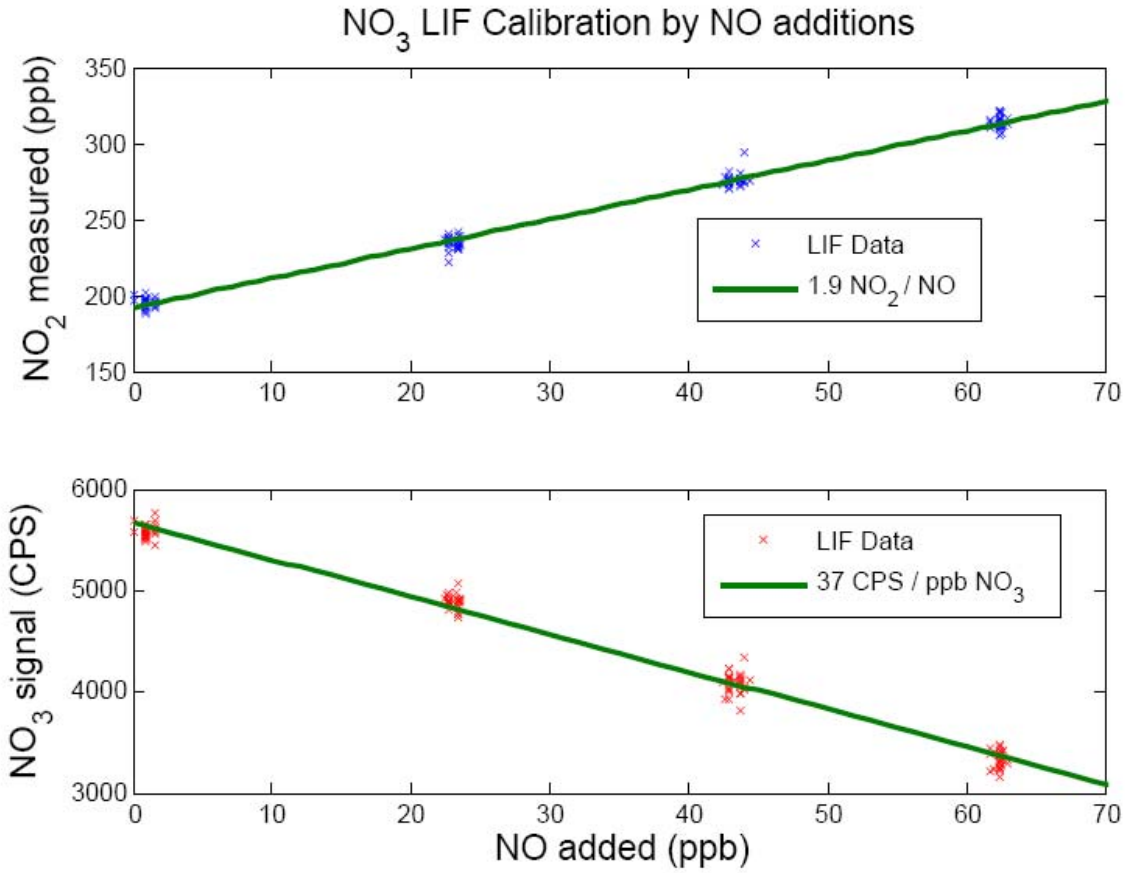

Figure 3. Calibration of the instrument including measurement of the NO_2 produced by titration of NO_3 with NO and simultaneous measurement of NO_3. The expected slope is 2 NO_2 per NO added and 1.9 is observed.

3.4 Field operation

A two channel instrument based on the testing and optimization described above was assembled in a field worthy package. Briefly, the entire laser system and detection module were mounted

as high as possible at each site and connected to vacuum pumps and electronics at the ground. A computer for control and data storage was used to operate the instrument remotely. Maintaining a stable background count required precise control over temperature fluctuations in the instrument package, because these fluctuations cause degradation in the laser alignment into the multi-pass cells. The instrument package was thermally stabilized using fans and heaters. The stabilization was most effective when ambient conditions were changing slowly during the night. Achieving optimal sensitivity required daily realignment of the laser system because the thermal fluctuations during the daytime caused significant alignment drifts. We tuned the laser alignment just after sunset each evening and did not perform any further adjustment until the next evening. During the latter half of the campaign, the laser alignment was more stable and there were number of evenings when the alignment was stable and no adjustments were required.

3.5 Summary

After establishing operational procedures as outlined in detail above, the Berkeley NO_3/N_2O_5 instrument is capable of routine operation in the laboratory setting. In a field setting, the requirement of outdoor operation results in exposure to large temperature variations that still cause laser alignment drifts. Correcting for these drifts requires daily attention while it is dark outside to maintain optimal sensitivity, although future efforts at thermal stabilization should be able to make the instrument operator free for weeks at a time.

The detection limit of the instrument depends on two factors. First the signal rate and second the accuracy to which we know the instrument zero. Our measurements show that typical signal rates for the instrument are about 36 counts/s/ppb as shown in Figure 3. We showed we know the zero to 0.1 counts or approximately 3ppt after a half hour of averaging. The uncertainty in the zero is shot noise limited and thus varies as the square root of integration time. Averaging for 5 hours reduces the uncertainty in the zero to 1ppt. Taken together these numbers result in a typical instrument detection limit of 25 ppt in a minute of averaging, 4 ppt in a half hour of averaging and 0.8 ppt if we average over an entire 12 hour night.

4. Field measurements

We made measurements during three deployments each 4 weeks long. During the observing period our main focus was on maintaining high data quality, improving instrument performance, and developing preliminary data for review and analysis. In this section we describe the sites and measurements.

4.1 Blodgett Forest in summer

The UC-BFRS (38° 54′ 45″ N, 120° 39′ 27″ W, 1315 m ASL) is located on the western slope of Sierra Nevada Mountains and about 5 hours down wind of the suburban edge of Sacramento. There is a strong mountain valley circulation affecting the site with upslope flow from the west during the day and downslope flow from the northeast at night. The Sacramento urban plume begins to arrive at the site at noon and has its peak impact at sunset just as the wind direction inverses. There have been extensive measurements of VOC, NO_x, O_3, CO, CO_2, and meteorological parameters at this site over the last 10 years providing context for interpreting the new NO_3 and N_2O_5 measurements. The Berkeley NO_3/N_2O_5 LIF instrument was mounted

on a walk up tower at 14 m 5 m above the top of the ponderosa pine plantation's canopy. Figure 4 shows a satellite image of the site location. Figure 5 presents pictures of the instrument, the tower and the local terrain as seen from the tower.

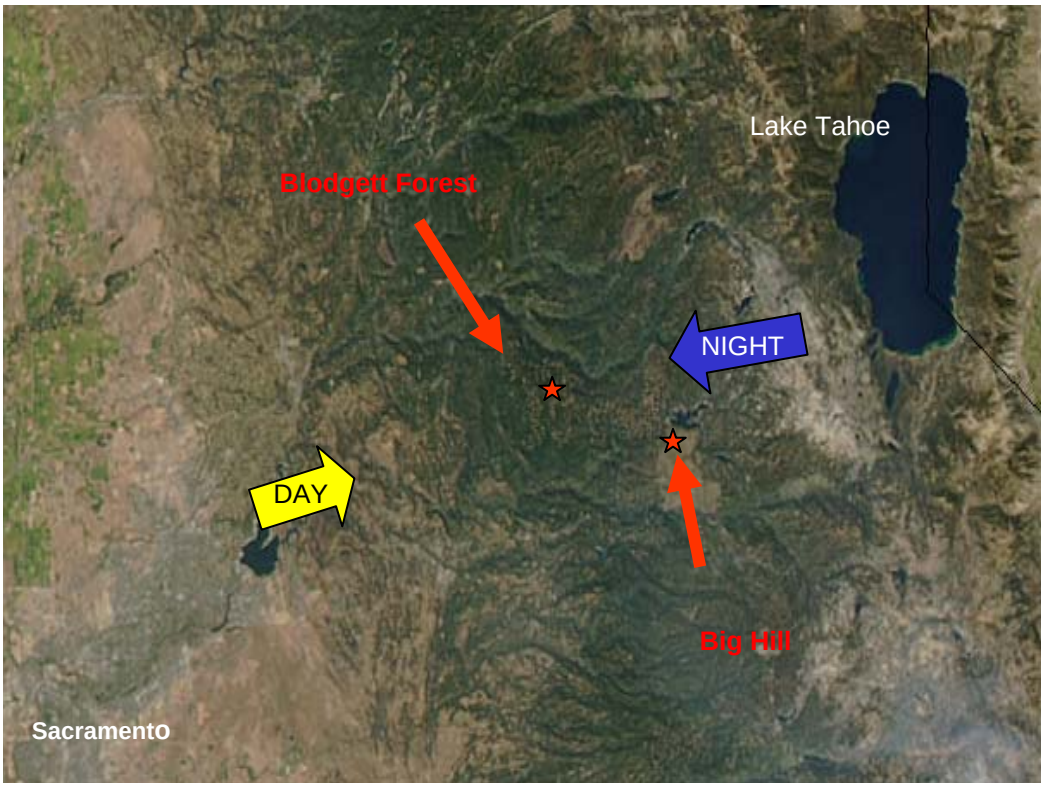

Figure 4. Satellite photograph of UC-BFRS and the surrounding region. Daytime and nighttime wind directions are marked along with the locations of UC-BFRS, Sacramento, the Big Hill monitoring site and Lake Tahoe.

Measurements of the sum of NO_3+N_2O_5 at Blodgett Forest during the summer phase (August 16-September 2) are shown in Figures 6 and 7. Figure 6 is a time series showing all of the nighttime measurements.

$$2 \times \sqrt{S^2 + B^2}, S = \sqrt{\frac{\text{mean of signal}}{\text{number of data points}}}, B = \sqrt{\frac{\text{mean of background}}{\text{number of data points}}}$$

Figure 7 shows mean value for each half hour. The error bar shown on this figure represents the range of the central 68 % of the data at the hour of day and is typical of the variance in the data set. The nighttime mean is 4 ± 1.5 ppt. The results are consistent with a rough estimate of 1 ppt precision of the mean for each half hour in the 20 day average. There is a slight hint that there is a 5-6 ppt mixing ratio during the first half of the night followed by decrease to 3-4 ppt mixing ratio after 2 AM. This decrease follows the decrease in NO_2 and O_3 over the night shown in Figure 8. Concentrations of NO_3 were not distinguishable from zero.

Figure 5. (Upper Left Panel) Photo showing the NO_3/N_2O_5 LIF instrument mounted on the side of the UC-BFRS tower. (Upper Right Panel) A view from the tower. Heights and species of the trees are monotonous. (Lower Panel) Photo showing a close up of the instrument (the silver shiny box to the right) on the tower.

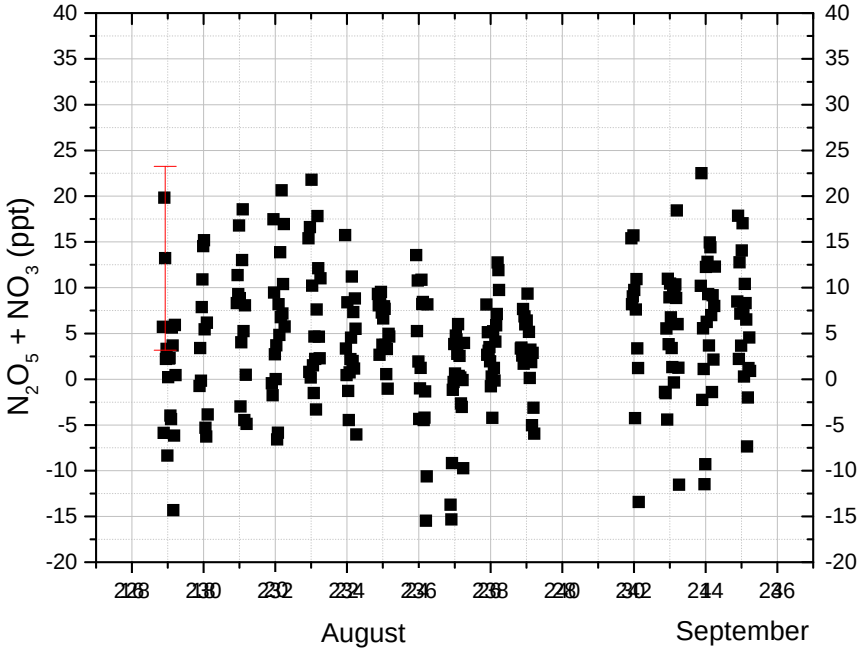

Figure 6. Observations of $N_2O_5 + NO_3$ at BFRS (points each 30-minutes) from August 16 – September 2, 2006. Example of error bars is presented. See text for the detailed explanation of error bars.

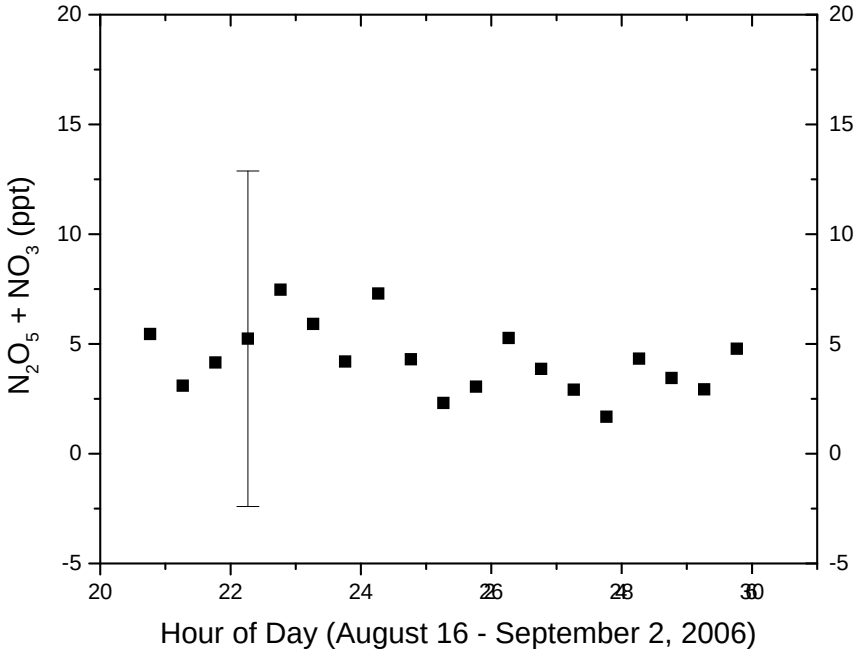

Figure 7. Observations of $N_2O_5 + NO_3$ at BFRS vs. time of day. The points are averaged from August 16 – September 2, 2006 at 30 min intervals. The error bar shown is typical of the variance of the central 68% of the data.

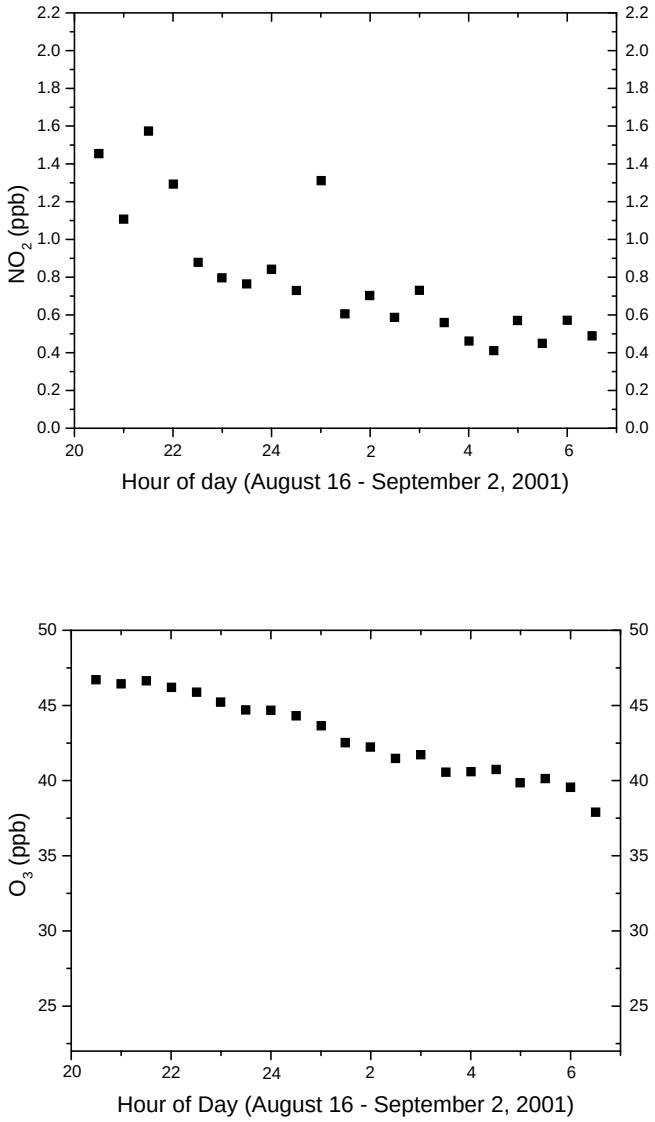

Figure 8. 30-minute observations (means) of (Upper Panel) NO_2, and (Lower panel) O_3 during the same time of year in 2001 at BFRS.

4.2 Blodgett Forest in late fall

Measurements of the sum of NO_3+N_2O_5 at Blodgett Forest during the late fall phase (November 5 -December 2) are shown in Figures 9 and 10. Figure 9 is a time series showing all of the nighttime measurements. Interruptions are due to rain and power failures at the site. Figure 10 shows the variation with time of night in half hour averages over the campaign The error bars shown on these figures represent the range of the central 68 % of the data at that hour of day and is typical of the variance in the data set. The concentrations of the NO_3+N_2O_5 sum average 4±1.5 ppt. Again as in the summer there is a slightly higher concentration earlier in the night.

Concentrations of NO_3 were not distinguishable from zero. The production rate for $N_2O_5 + NO_3$ changed little in the Fall as increases in NO_2 were offset by decreases in O_3. Nighttime temperatures were 10-20°C during the summer and 0-10 °C for Fall. Figure 11 shows NO_2 and O_3 at this site for the year 2000 as a guide to estimating the NO_3 production rate.

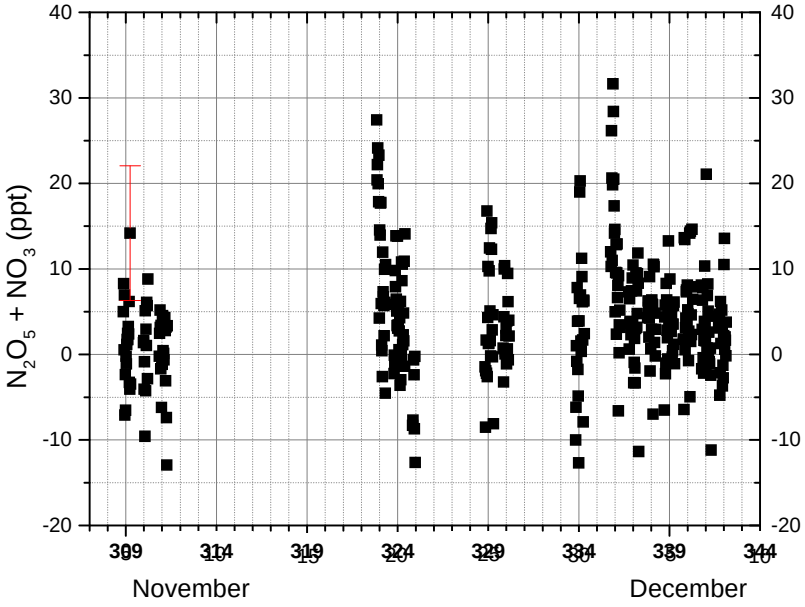

Figure 9. Observations of $N_2O_5 + NO_3$ at BFRS from November 4-December 8, 2006.

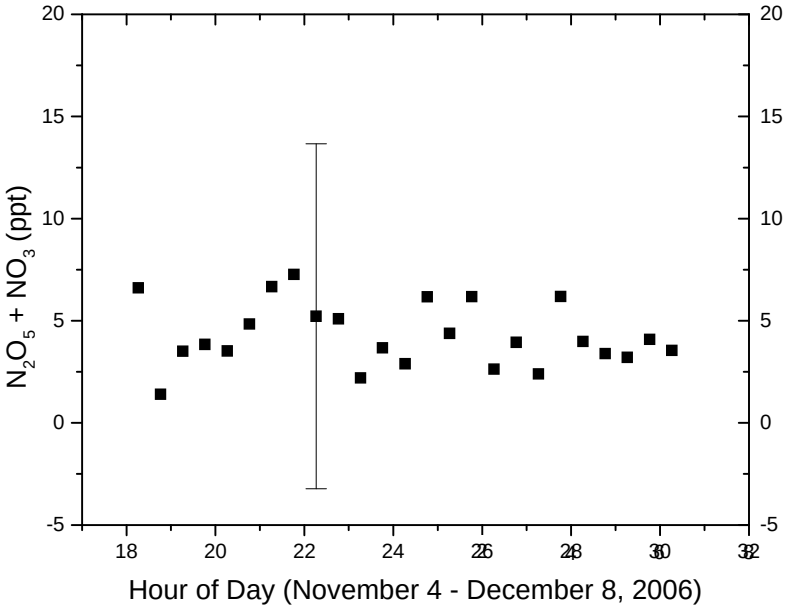

Figure 10. Observations of $N_2O_5 + NO_3$ at BFRS vs. Time of day (points each 30-minutes) from November 4-December 8, 2006.

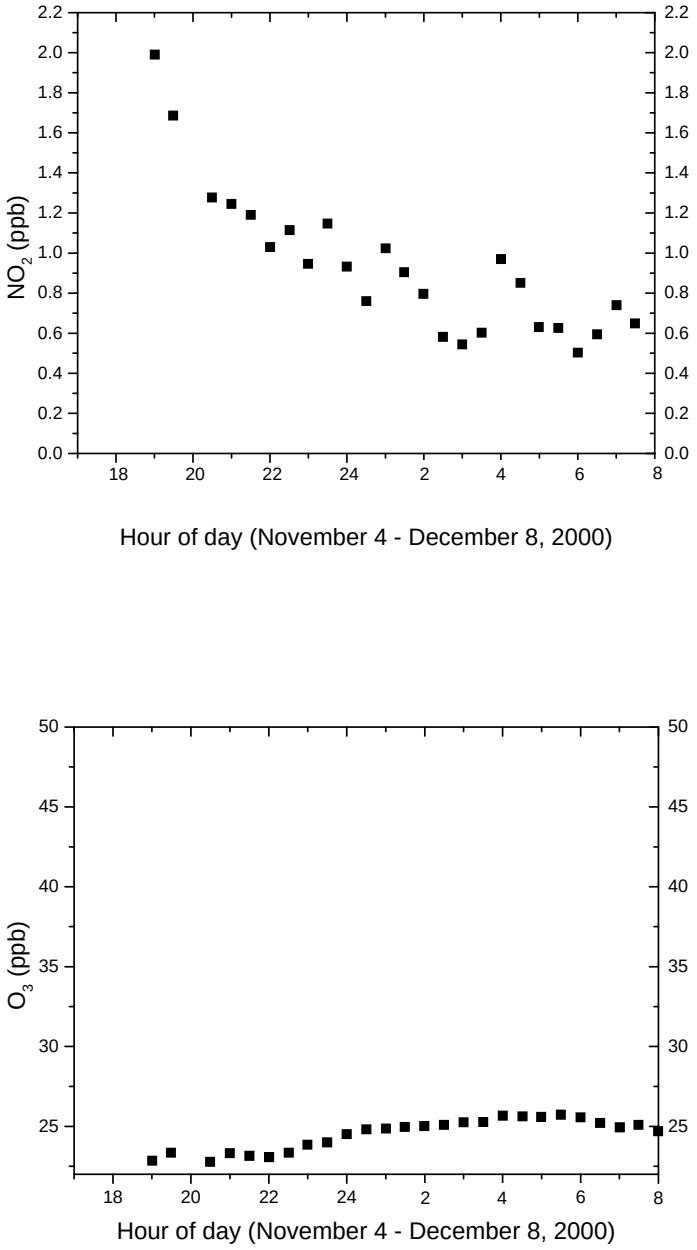

Figure 11. 30-minute observations (means) of (Upper Panel) NO_2, and (Lower panel) O_3 during the same time of year in 2000 at BFRS.

4.3 Arvin in early spring

With the help of John Karlik and a farm owner Steve Murray, we were able to identify a suitable location in the southern San Joaquin valley near Arvin (Figure 12,13,14). The site was a privately owned orchard 4 km east of downtown Arvin (population is 13,000), and about 38 km southeast of Bakersfield (population of 250,000). The Arvin-Bear-Mountain Blvd. CARB site (Site # 15247) is located approximately 2 km east from the orchard. Crops on the orchard included orange trees (25% land cover), almond trees and cherry trees. Beginning on March 10th, the almond trees started to bud. The prevailing wind during the day was from the direction of Bakersfield, but during the night the wind direction was mainly from north east to south east (Figure 15).. Traffic in the region was low and highways were far enough away that NO emissions at the highways would have been converted to NO_2 well before reaching the orchard site. The instrument was located on top of a shipping container (Figure 14).

Figure 12. Map of California, Arvin is indicated by the red star (From mapquest).

Figure 13. Satellite photograph (Google Earth) showing the vicinity of the Arvin observation site and the Arvin Bear Mountain Blvd. CARB site.

Figure 14. (Upper panel) Photo of NO_3/N_2O_5 LIF instrument mounted atop the trailer at the Arvin observation site. (Lower panel) Photo of the site from the instrument platform.

Measurements of the sum of NO_3+N_2O_5 at the Arvin site during the early Spring phase (March 1 - March 30) are shown in Figures 16, 17, 19-21. Figure 16 is a time series showing all of the nighttime measurements. Interruptions are due to rain and power failures at the site. In contrast to the UC-BFRS observations the measurements were well above the detection limit. Figure 17 shows the variation with time of night in half hour averages over the entire campaign. The error bar shown on this figure represents the range of the central 68 % of the data at the hour of day and is typical of the variance in the data set. Figure 18 provides NO_2 and O_3 for use in estimating NO_3 production rates. Figures 19, 20, and 21 provide examples of the variation of $NO_3 + N_2O_5$, NO_2 and wind direction on three different nights. Correlations among the different quantities are evident in the figures.

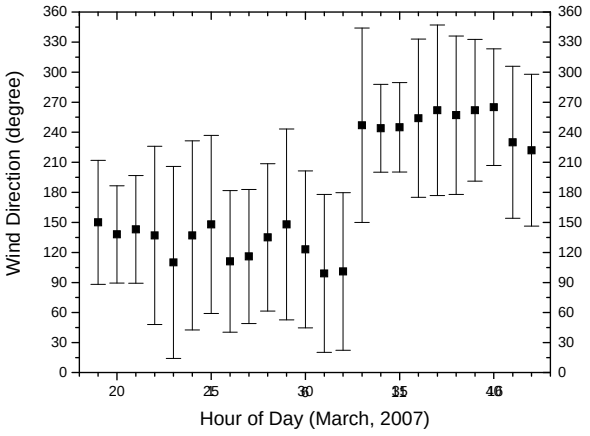

Figure **15**. Observations of wind direction at the Arvin Bear Mountain Blvd. CARB site vs. Time of day from March 1-March 31, 2006. Points represent the mean and the bars the extent of the central 68% of the observations.

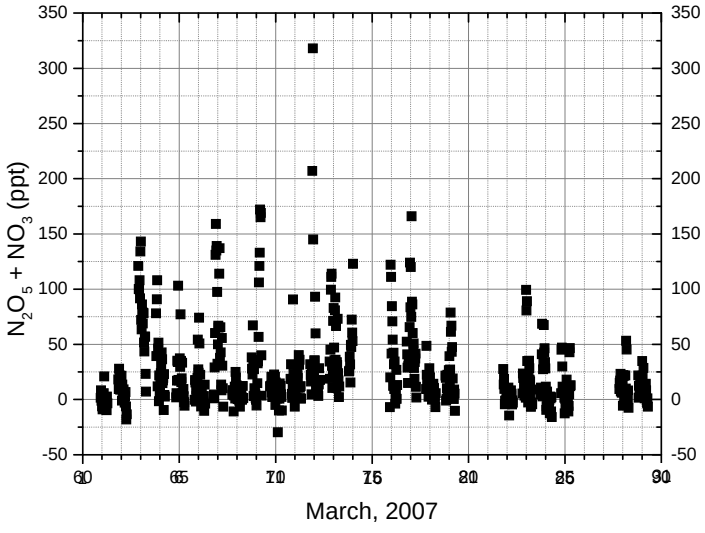

Figure 16. Observations of N_2O_5 + NO_3 at Arvin from March 1- March 29, 2007.

The temporal structures varied on different nights indicating that the source of air to the site experienced a varied history. Concentrations reached as high 300 ppt and values in the range of 100-150 ppt were not unusual. Concentrations of NO_3 were not distinguishable from zero. This is not surprising as the predicted ratio of N_2O_5 to NO_3 at this site is about 20:1. As we discuss below, the higher concentrations we observe here compared to UC-BFRS are mostly because of larger NO_2 concentrations at this site. In general, concentrations rose during the first few hours of darkness, then were constant for 4-5 hours before decreasing (Figure 17).

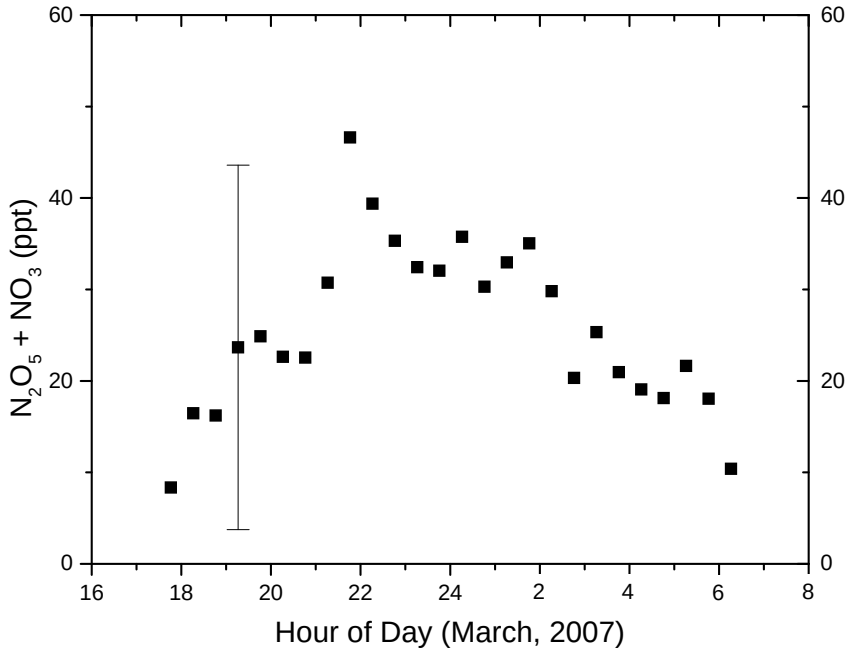

Figure 17. Observations of $N_2O_5 + NO_3$ at Arvin vs. Time of day (points each 30-minutes) from March 1-March 31, 2006. The symbols are the mean values and the bar an example of the variance of the central 68% of the data.

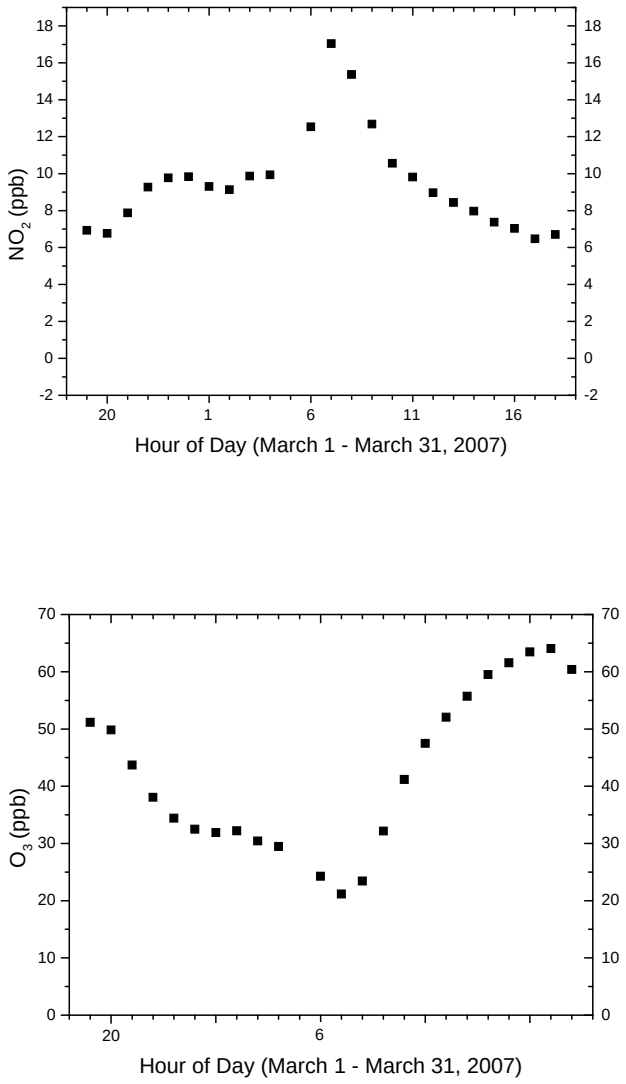

Figure 18. 1 hour observations (means) of (Upper Panel) NO_2, and (Lower panel) O_3 during the same time of year in 2006 at CARB Arvin site.

4.4 Aerosol measurements

We operated a particle counter (CI-500, Climet Instruments Co.) at Blodgett in late Fall 2006 and at the Arvin site. Figure 22 shows the size dependence of the calculated particle surface area inferred from the observations at Arvin. Since the CI-500 particle counter has a lower size limit of 0.5 μm diameter, and much of inferred surface area is carried by smaller particles, there is considerable uncertainty in the surface area estimate. The figure indicates that 10- 40 % of the surface area is in the size range observed using this instrument—we thus estimate the derived surface is uncertain to about a factor of 2. Figure 23 and 24 are time series of aerosol surface area above 0.5 μm particle diameter both in Blodgett in winter 2006 and early spring in March of the two deployments where we made measurements. We observed a surface area above of

0.5 μm particle diameter of 20-150 $\mu m^2/cm^3$ and estimate that the total surface area was in the range 300 – 700 $\mu m^2/cm^3$.

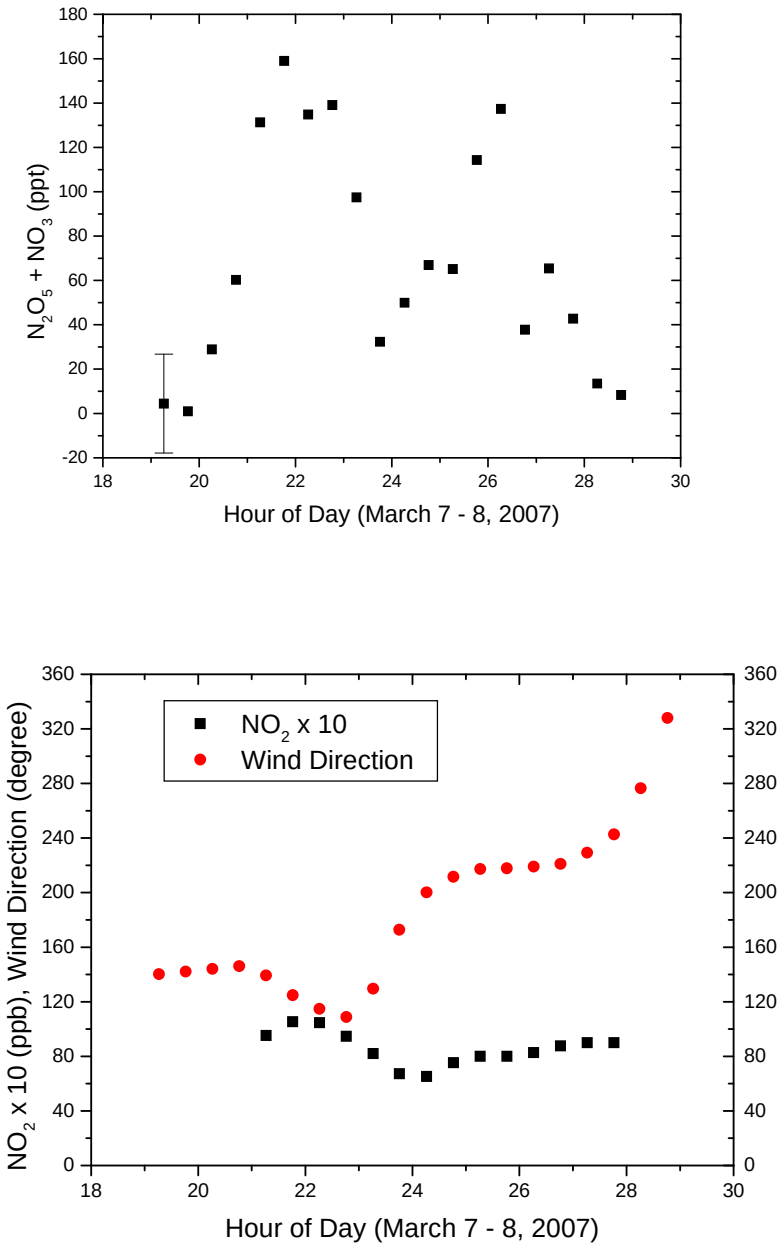

Figure 19. (Upper Panel) $N_2O_5 + NO_3$ concentration (30 min average), (Lower Panel) NO_2 and wind direction over March 7 – 8 night. Examples of error bars are presented. See text for the detailed explanation of error bars.

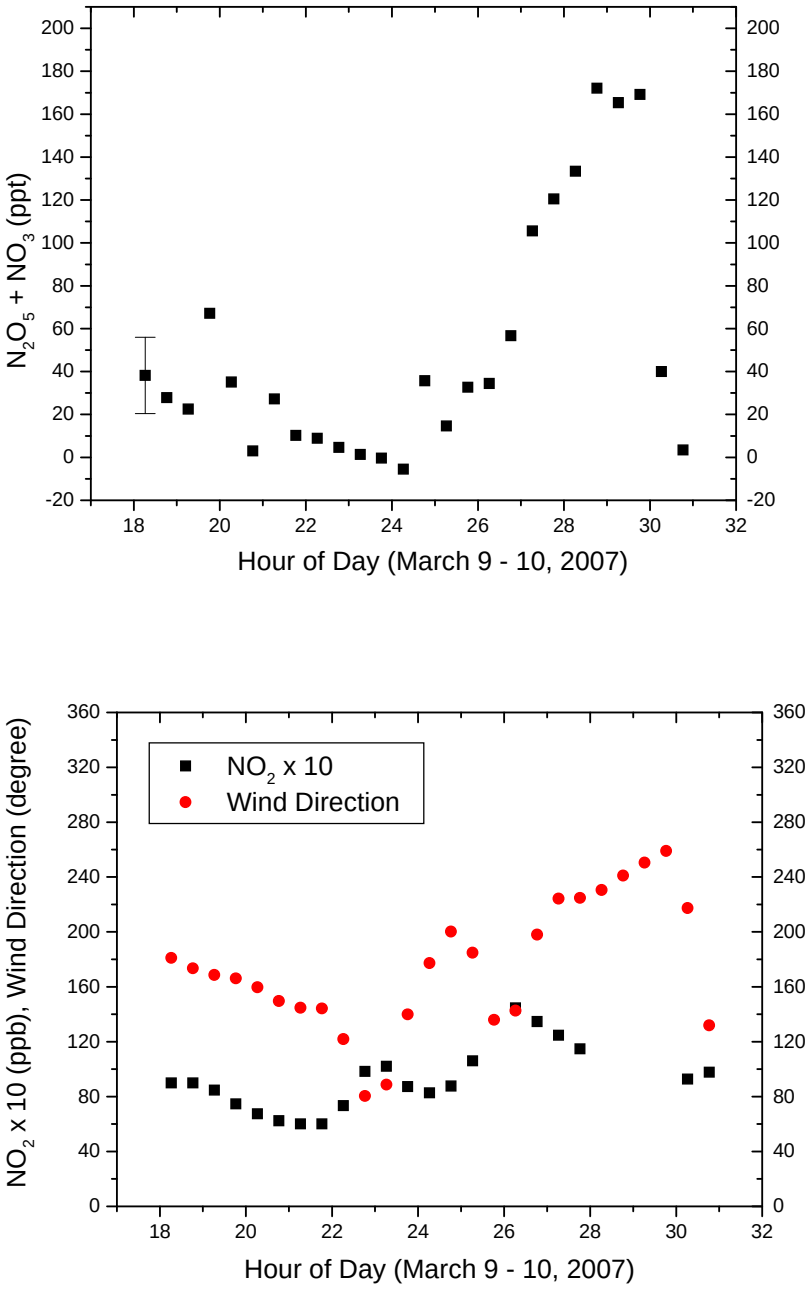

Figure 20. (Upper Panel) N_2O_5 + NO_3 concentration (30 min average), (Lower Panel) NO_2 and wind direction over March 9 – 10 night.

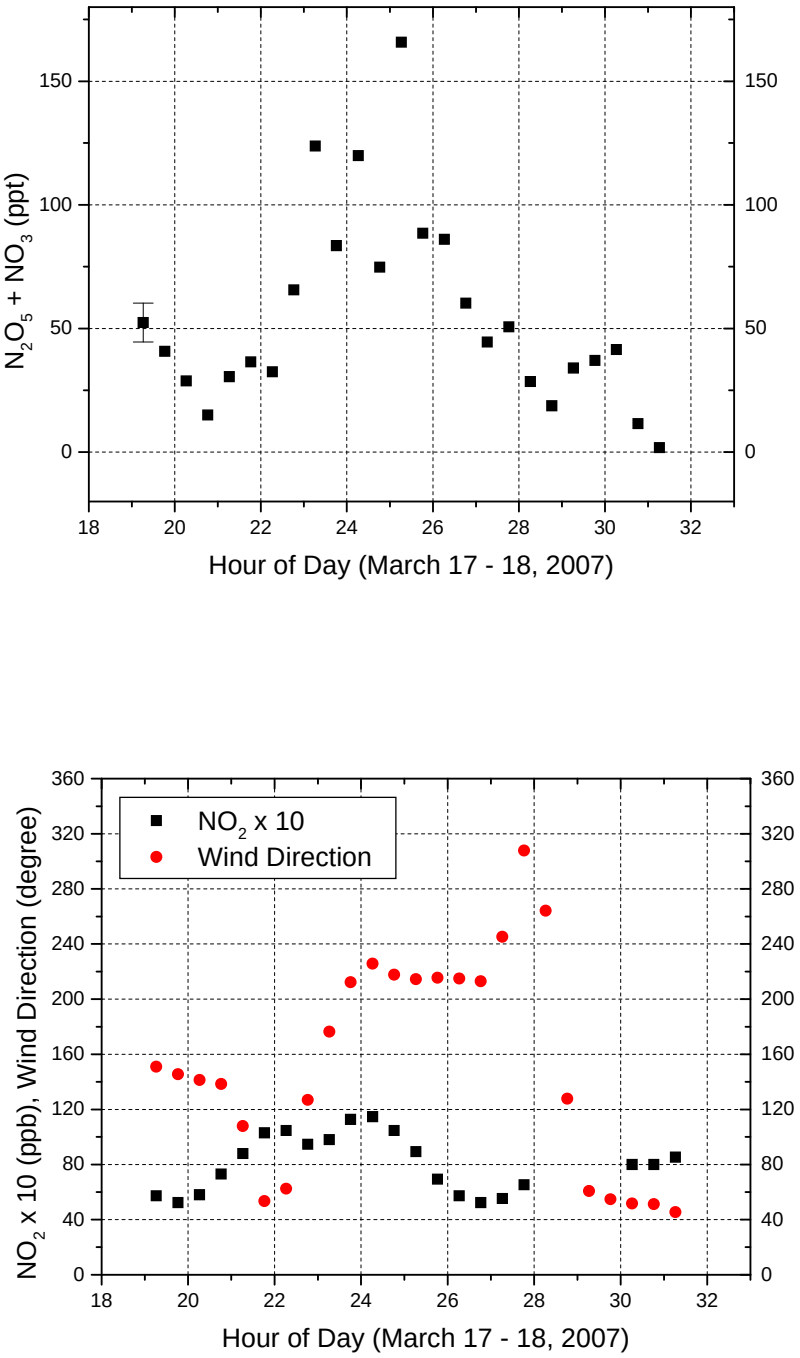

Figure 21. (Upper Panel) $N_2O_5 + NO_3$ concentration (30 min average), (Lower Panel) NO_2 and wind direction over March 17 – 18 night.

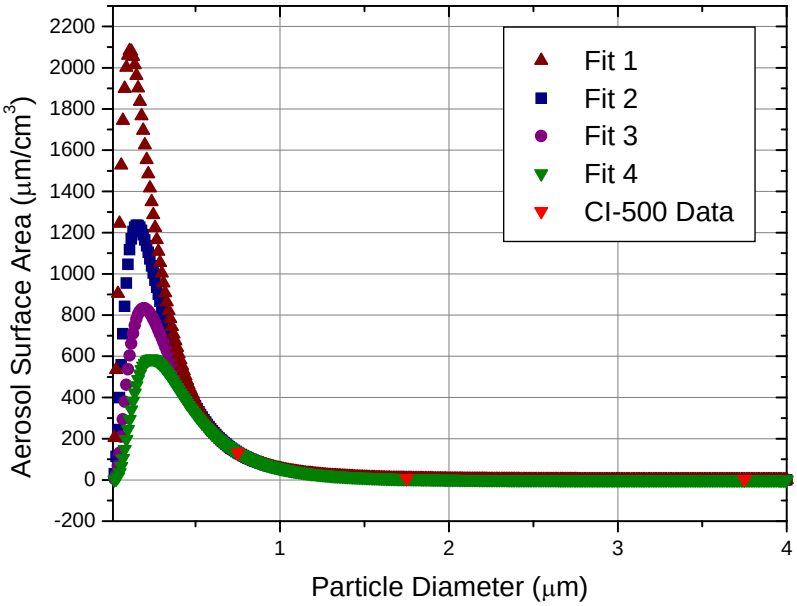

Figure 22. CI-500 particle number data were converted to surface area assuming a single diameter in each bin. Examples of various fits are presented. Total surface areas calculated from the fits are 1; 659 $\mu m^2/cm^3$, 2; 473 $\mu m^2/cm^3$, 3; 366 $\mu m^2/cm^3$, 4; 290 $\mu m^2/cm^3$.

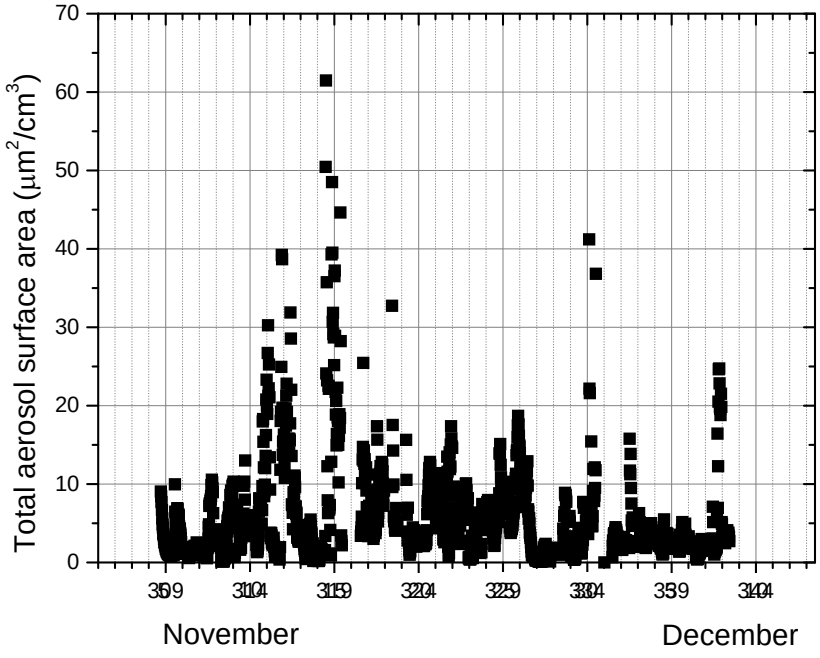

Figure 23. 30 min. average of surface area of particles larger than 0.5 μm in diameter at BFRS in Fall 2006.

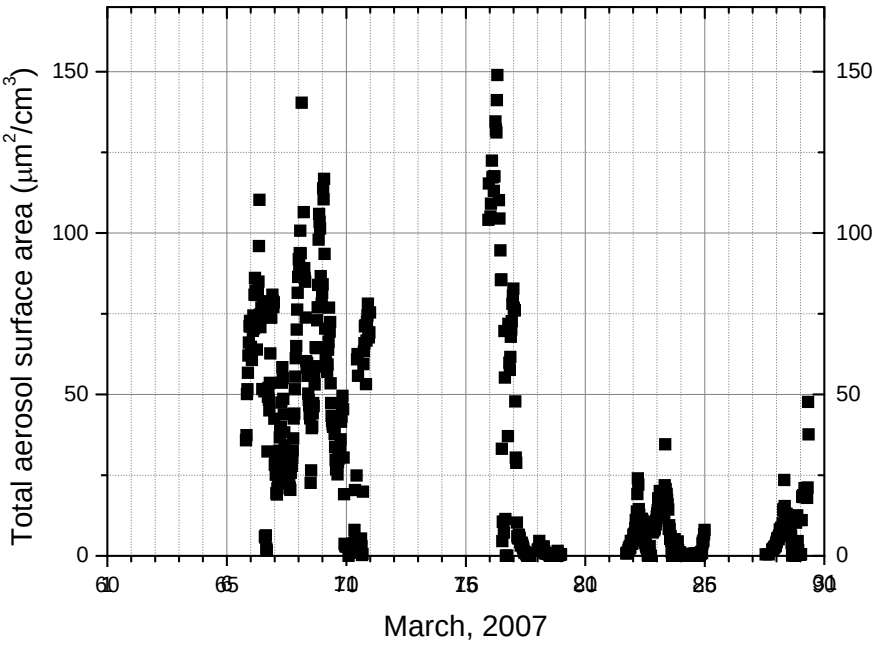

Figure 24. 30 min. average of surface area of particles larger than 0.5 μm in diameter at Arvin in March 2007.

5. Discussion

As we described in section 2 our understanding of the production rate of NO_3 and the equilibrium between NO_3 and N_2O_5 based on laboratory observations are believed to be accurate. Thus if O_3 and NO_2 are measured (or accurately modeled) then the source of NO_3 and N_2O_5 and the ratio of NO_3 to N_2O_5 will be accurately modeled. In contrast, there are major uncertainties in our understanding of the processes by which NO_3 and N_2O_5 are converted to other nitrogen oxides and removed from the atmosphere. We focus our analysis of the field measurements we described above on the question of loss rates.

We determine the chemical lifetime of the sum of NO_3+N_2O_5 based on assumptions that these two chemicals are in equilibrium with each other and in steady state with their sources and sinks. These assumptions are supported by prior observations and analysis by Brown et al. [2003] who show steady-state to be a good approximation when the N_2O_5 and NO_3 lifetimes are short. The time rate of change for $[NO_3]$ and $[N_2O_5]$ are given by the following equations:

$$\frac{d[NO_3]}{dt} = \quad 0 \quad = k_1[NO_2][O_3] + k_b[N_2O_5] - k_f[NO_2][NO_3] - k_x[NO_3] \tag{4}$$

$$\frac{d[N_2O_5]}{dt} = \quad 0 \quad = k_f[NO_2][NO_3] - k_b[N_2O_5] - k_y[N_2O_5] \tag{5}$$

$$\frac{d[N_2O_5 + NO_3]}{dt} = \quad 0 \quad = k_f[NO_2][NO_3] - k_x[NO_3] - k_y[N_2O_5] \qquad (6)$$

where k_f is the effective bimolecular rate constant for the association reaction of NO_2 and NO_3 (1.3×10^{-12} cm^3 molecule^{-1} s^{-1} at 278 K), k_b is the rate constant for N_2O_5 decomposition, and k_x and k_y are the 1st order rate constants for NO_3 and N_2O_5 irreversible loss, respectively.

$$\tau_{SS}(N_2O_5 + NO_3) \equiv \frac{[N_2O_5 + NO_3]}{k_1[NO_2][O_3]} = \frac{[N_2O_5 + NO_3]}{k_y[N_2O_5] + k_x[VOC][NO_3]} = \frac{1+\alpha}{k_y + k_x[VOC]\alpha} \qquad (7)$$

where K_{eq} is the equilibrium constant for reaction 2 and $\alpha = \frac{[NO_3]}{[N_2O_5]} = \frac{1}{K_{eq}[NO_2]}$. This equation relates the lifetime to the production rate for N_2O_5, $k_1[NO_2][O_3]$, or to the loss rates, k_x and k_y.

5.1 UC-BFRS

There were not simultaneous measurements of NO_2 or O_3 at UC-BFRS. However, nocturnal production rates of NO_3 and N_2O_5 can be estimated from prior measurements of NO_2 and O_3 at the UC-BFRS site since several years of measurements show there is relatively little interannual variability in the NO_2 or O_3. The NO_3 production rate is calculated to be approximately 0.9 ppt-min^{-1} (summer) 0.5 ppt-min^{-1} (fall).

Using the measured NO_2 and the equilibrium constant for reaction 2, we estimate that N_2O_5 and NO_3 are about equal in the summer (T=10-20 ºC) and that 90% of the sum of NO_3+N_2O_5 was N_2O_5 during the fall sampling period (T=0-10 ºC). Assuming steady state, the lifetime of the sum of NO_3+N_2O_5 is equal to the concentration divide by this production rate (0.9 ppt-min^{-1} in the summer and 0.5 ppt-min^{-1} in the late Fall). Using the measured concentrations of 4 ppt in both seasons we calculate N_2O_5 +NO_3 lifetimes of ~ 4 minutes in summer and ~ 14 minutes in fall

If we assume this is entirely due to reactions of NO_3 with alkenes we can estimate the alkene concentration. Using a typical rate constant for such reactions, k= 5 x 10^{-12} cm^3/molecule/s and and the calculated ratio of NO_3/N_2O_5 of 1:1 in summer and 1:10 in the Fall, the required alkene concentrations are 1.5 x 10^9 molec/cm^3 (80 ppt) in summer and 2.3 x 10^9 (120ppt) in the fall. These are the same order of magnitude as the observations which were 250 ppt in summer and 70 ppt in Fall.

The results do not rule out a role for aerosol reactions or mixing, but do suggest that VOC reactions are the primary sink for NO_3 + N_2O_5 in the surface layer.

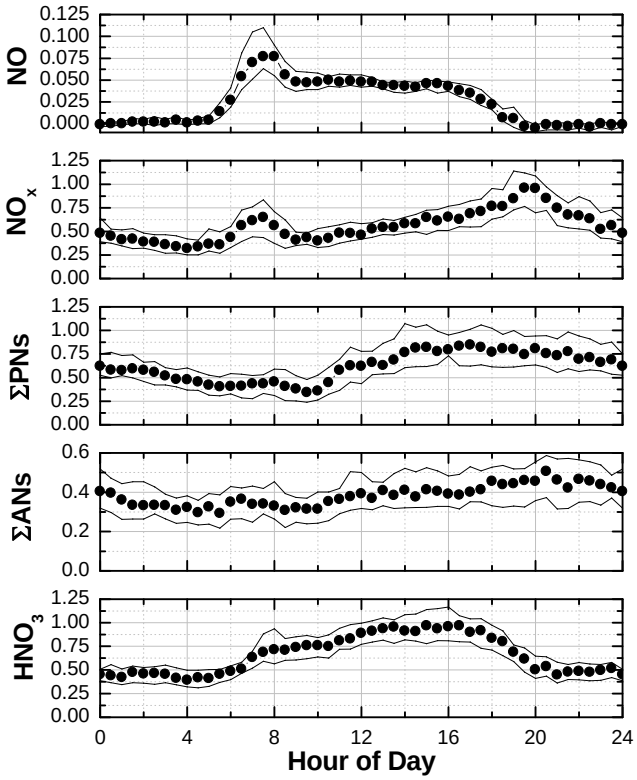

Figure 25. Measurements of NO, NO_x, ΣPNs, ΣANs and HNO_3 vs. time of day during May-September 2001 at UC-BFRS. The symbols are the median values and the lines bound the central 68% of the data.

Rapid losses due to NO_3 reactions are consistent with prior observations of other nitrogen oxides at UC-BFRS. Figure 25 shows the median and the range of the central 68% of the observed mixing ratios of NO, NO_x, ΣPNs, ΣANs, and HNO_3 at UC-BFRS vs. time of day during the summer (May-September) 2001. The diurnal cycle in NO_x, with a peak in the early evening is the typical pattern at UC-BFRS. Upslope flow during the day transports the Sacramento urban plume to the site. Down slope flow at night cleanses the site. The observations show that from 8PM to 5AM, NO_x decreases by a factor of 3 (from 1 to 0.30 ppb), both ΣPNs (0.75 to 0.35 ppb) and ΣANs (0.5 to 0.25 ppb) decrease by a factor of 2, while HNO_3 remains nearly constant at 0.4 ppb. One possible explanation for this pattern is that NO_2 is removed by conversion to NO_3 which reacts rapidly to produce HNO_3 and ΣANs, both of which deposit. The decrease in ΣPNs is the result of thermal decomposition followed by RO_2 reactions. If this is correct, then the high nighttime values of HNO_3 and ΣANs imply there must be large yields of both ΣANs and HNO_3 during the reaction of NO_3 with the biogenics present at UC-BFRS—a conjecture that should be tested with detailed mechanistic calculations such as would be possible using the Master Chemical Mechanism [Zador et al. 2006; Sommariva et al., 2007]. It is interesting that the NO_x loss chemistry appears to be less effective within the residual layer. During the mixing of the surface layer with the residual layer above it (note the rise in NO_x, ΣANs and HNO_3 beginning at 6AM) NO_x mixing ratios increase more than do those of HNO_3, ΣANs, or ΣPNs suggesting that chemistry in the nocturnal and residual layer does not result in NO_x loss or HNO_3 production with the same efficacy as occurs within the surface layer. This inference is consistent with direct measurements by Brown et al.[2007] showing much slower

chemical losses of NO_3+N_2O_5 above the surface layer near Boulder Colorado. It implies that the biogenic alkenes at night are primarily confined to the surface layer and that losses of NO_3+N_2O_5 on aerosol within the residual layer are slow. It is also consistent with our inference that downward transport can possibly contribute to the observed NO_3 + N_2O_5 mixing ratios.

Figure 26 shows measurements of NO, NO_X, ΣPNs, ΣANs and HNO_3 vs. time of day during November-December 2001 at UC-BFRS. The symbols are the median values and the lines bound the central 68% of the data. The concentrations are low with small diurnal and nocturnal variation. The only strong variation is a decrease in NO_2 at night. This is consistent with removal by NO_3 chemistry but requires more rapid removal of any HNO_3 or ΣANs produced in winter than in summer. Alternatively the NO_2 decrease could be primarily due to transport.

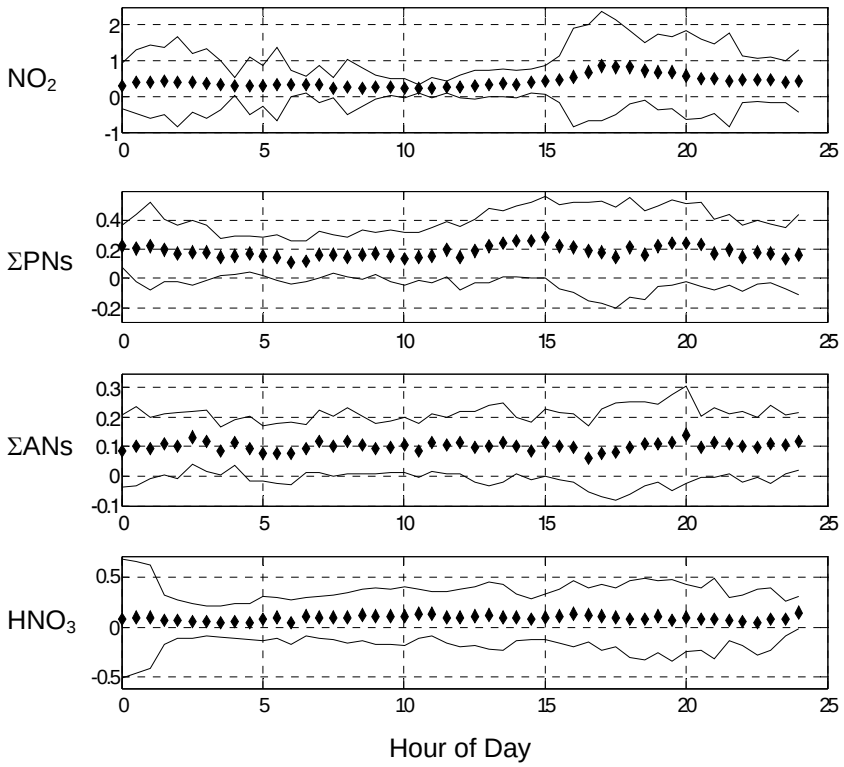

Figure 26. Measurements of NO, NO_X, ΣPNs, ΣANs and HNO_3 vs. time of day during November-December 2001 at UC-BFRS. The symbols are the median values and the lines bound the central 68% of the data.

5.2 Arvin

The 25 ppt average nighttime mixing ratio of N_2O_5 that we observed at Arvin corresponds to a lifetime of approximately 4 minutes. Since the lifetime is the same as that of UC-BFRS, the fact that the concentration is higher than at Blodgett Forest is almost entirely due to the 8 times higher NO_2 at the site. Surprisingly, even at this Central Valley site aerosol removal processes are not likely to be important. The N_2O_5 loss rate constant (k_{het}) due to heterogeneous uptake onto aerosol can be expressed as

$$k_{het} = \tau^{-1}(N_2O_5) = \gamma A\bar{c}/4 \quad (10)$$

where γ is the uptake coefficient of N_2O_5 and is a function of the aerosol composition, *A* is the surface area density, and $\bar{c}$ is the mean molecular speed of N_2O_5.

For aerosol reactions to be completely responsible for the observed N_2O_5+NO_3 lifetimes of 4 minutes requires the product of aerosol surface area density ($\mu m^2\ cm^{-3}$) and γ (unitless) to be about 100 $\mu m^2\ cm^{-3}$. For example for the highest surface area we estimate might have been present at Arvin 700 $\mu m^2\ cm^{-3}$, γ of 0.15 would be required. This value for γ is more than 10 times the peak value of 0.017 reported by Brown et al [2006] for sulfate aerosol and smaller γ values are likely to be associated with NH_4NO_3 aerosol. Thus it is likely that aerosol reactions represent 1-10 % of the removal of N_2O_5 +NO_3 at the Arvin site. Based on this fact we estimate the VOC at Arvin as we did for UC-BFRS (using k for NO_3 +alkenes of k= 1.2 x 10^{-11} cm^3/molecule/s). The result is an estimate of 300 ppt of alkenes. These values are not surprising for observations above an orchard.

While, in general, reactions of N_2O_5 on aerosol were slow compared to reactions of NO_3 with VOC, there were individual events where N_2O_5 was as much as 10 times larger than the mean without a corresponding increase in NO_2. It is likely that there were lower alkene concentrations in these air masses and that aerosol processes were important at these times at the Arvin site.

6. Conclusions and Recommendations

The experiments described here affirm that the LIF technique is capable of making in situ measurements of NO_3 and N_2O_5. We have demonstrated sensitivity of 1 ppt for 5 hour averages and 25 ppt/min in the field.

Recent observations by other researchers show we have an excellent understanding of the production of NO_3 and N_2O_5 and their equilibrium. What we still need to learn about from a combination of laboratory, field measurements and modeling are the fate of NO_3 and N_2O_5 once they have been produced. The issue is important because it is these processes that determine both the extent to which O_x is removed at night, the extent to which NO_x survives to accumulate over several days and the extent to which NO_3 chemistry leads to SOA. The relative importance of these different process varies strongly with height above the surface. The results of the field experiments described here and other recent field experiments from the NOAA and University of Alaska groups show that measurements within the surface layer do teach us some of the important things we need to learn about nocturnal nitrogen oxide chemistry. However it is also increasingly clear that what occurs higher in the nocturnal and residual layers is important.

In the research conducted here we show that in two different regions of California, VOC reactions are the predominant sink of NO_3 and N_2O_5. We have been informed that the ARB's planning and Technical Support division plan to use these observations in their ongoing assessment of these issues. The products of these VOC reactions –whether NO_2, organic nitrates

of HNO_3 are not well known. As a result, we can not say with confidence whether nocturnal nitrogen oxide chemistry is a source of aerosol organic or inorganic nitrate. We can say with confidence that chemistry of these species on aerosol surfaces within the meteorological surface layer is not a major source of HNO_3. However, production of HNO_3 is likely very efficient in NO_3 + VOC reactions. It remains to be seen whether this fact is also the case in the nocturnal and residual layers and other modeling and field experiments will be needed to quantify the role of these processes.

Among the next steps in research on nocturnal chemistry should be simultaneous measurements of NO, NO_2, O_3, NO_3, N_2O_5, aerosol size distributions and composition, the widest suite of alkenes possible, both total and speciated peroxynitrates, both total and speciated alkyl- and nonperoxy multifunctional nitrates and HNO_3. It is only with this full complement that we will be able to test current and newly developing ideas about the role of NO_3 and N_2O_5 chemistry in the production of aerosol and removal of NO_x. It is also worth noting in this context that reactions of NO_3 with biogenics are known to be some of the strongest sources of SOA. Ideally the measurements would be made on a platform that allows routine access well above the surface layer or from an aircraft that can obtain repeated profiles at night. In addition to these field measurements our understanding would be advanced by flow tube and chamber studies of the nitrogen oxide and aerosol products of reactions of NO_3 with alkenes. Branching ratios for formation of organic nitrates, NO_2 and HNO_3 should be measured for a wide variety of alkenes.

7. References

Ayers, J. D., R. L. Apodaca, et al. (2005). "Off-axis cavity ringdown spectroscopy: application to atmospheric nitrate radical detection." Applied Optics **44**(33): 7239-7242.

Ball, S. M., J. M. Langridge, et al. (2004). "Broadband cavity enhanced absorption spectroscopy using light emitting diodes." Chemical Physics Letters **398**(1-3): 68-74.

Biggs, P., C. E. Canosamas, et al. (1994). "Investigation into the kinetics and mechanism of the reaction of NO_3 with CH_3O_2 at 298 K and 2.5 Torr a potential source of OH in the nighttime troposphere." Journal of The Chemical Society-Faraday Transactions **90**(9): 1205-1210.

Biggs, P., C. E. Canosamas, et al. (1995). "Rate constants for the reactions of C_2H_5, C_2H_5O and $C_2H_5O_2$ radicals with NO_3 at 298 K and 2.2 Torr." Journal Of The Chemical Society-Faraday Transactions **91**(5): 817-825.

Bitter, M., S. M. Ball, et al. (2005). "A broadband cavity ringdown spectrometer for in-situ measurements of atmospheric trace gases." Atmospheric Chemistry and Physics **5**: 2547-2560.

Brown, S. S., H. Stark, et al. (2002a). "Simultaneous in situ detection of atmospheric NO_3 and N_2O_5 via cavity ring-down spectroscopy." Review of Scientific Instruments **73**(9): 3291-3301.

Brown, S. S., H. Stark, et al. (2002b). "Cavity ring-down spectroscopy for atmospheric trace gas detection: application to the nitrate radical (NO_3)." Applied Physics B-Lasers and Optics **75**(2-3): 173-182.

Brown, S. S., H. Stark, et al. (2003a). "Applicability of the steady state approximation to the interpretation of atmospheric observations of NO_3 and N_2O_5." Journal of Geophysical Research-Atmospheres **108**(D17).

Brown, S. S., H. Stark, et al. (2003b). "Nitrogen oxides in the nocturnal boundary layer: Simultaneous in situ measurements of NO_3, N_2O_5, NO_2, NO, and O_3." Journal of Geophysical Research-Atmospheres **108**(D9).

Brown, S. S., J. E. Dibb, et al. (2004). "Nighttime removal of NO_x in the summer marine boundary layer." Geophysical Research Letters **31**(7).

Brown, S. S., T. B. Ryerson, et al. (2006). "Variability in nocturnal nitrogen oxide processing and its role in regional air quality." Science **311**(5757): 67-70.

Brown, S. S., W. P. Dube, et al. (2007). "High resolution vertical distributions of NO_3 and N_2O_5 through the nocturnal boundary layer." Atmospheric Chemistry And Physics **7**: 139-149.

Carslaw, N., J. M. C. Plane, et al. (1997). "Observations of the nitrate radical in the free troposphere at Izana de Tenerife." Journal of Geophysical Research-Atmospheres **102**(D9): 10613-10622.

Dubé, W. P., S. S. Brown, et al. (2006). "Aircraft instrument for simultaneous, in situ measurement of NO_3 and N_2O_5 via pulsed cavity ring-down spectroscopy." Review of Scientific Instruments **77**(3).

Dunlea, E. J., S. C. Herndon, et al. (2007). "Evaluation of nitrogen dioxide chemiluminescence monitors in a polluted urban environment." Atmospheric Chemistry And Physics **7**(10): 2691-2704.

Evans, M. J. and D. J. Jacob (2005). "Impact of new laboratory studies of N_2O_5 hydrolysis on global model budgets of tropospheric nitrogen oxides, ozone, and OH." Geophysical Research Letters **32**(9).

Geyer, A., B. Alicke, et al. (1999). "Comparison of tropospheric NO_3 radical measurements by differential optical absorption spectroscopy and matrix isolation electron spin resonance." Journal of Geophysical Research-Atmospheres **104**(D21): 26097-26105.

Geyer, A., B. Alicke, et al. (2001). "Chemistry and oxidation capacity of the nitrate radical in the continental boundary layer near Berlin." Journal of Geophysical Research-Atmospheres **106**(D8): 8013-8025.

Geyer, A. and J. Stutz (2004). "Vertical profiles of NO_3, N_2O_5, O_3, and NO_x in the nocturnal boundary layer: 2. Model studies on the altitude dependence of composition and chemistry " Journal of Geophysical Research-Atmospheres **109**(D16).

Goldstein, A. H., M. McKay, et al. (2004). "Forest thinning experiment confirms ozone deposition to forest canopy is dominated by reaction with biogenic VOCs." Geophysical Research Letters **31**(22).

Hanson, D. R. (1997). "Reaction of N_2O_5 with H_2O on bulk liquids and on particles and the effect of dissolved HNO_3." Geophysical Research Letters **24**(9): 1087-1090.

Heintz, F., U. Platt, et al. (1996). "Long-term observation of nitrate radicals at the Tor station, Kap Arkona (Rügen)." Journal of Geophysical Research-Atmospheres **101**(D17): 22891-22910.

Holzinger, R., A. Lee, et al. (2006). "Seasonal variability of monoterpene emission factors for a Ponderosa pine plantation in California." Atmospheric Chemistry and Physics **6**: 1267-1274.

Kim, B. S., P. L. Hunter, et al. (1992). "NO_3 Radical Studied by Laser-Induced Fluorescence." Journal of Chemical Physics **96**(6): 4057-4067.

Kurpius, M. R. and A. H. Goldstein (2003). "Gas-phase chemistry dominates O_3 loss to a forest, implying a source of aerosols and hydroxyl radicals to the atmosphere." Geophysical Research Letters **30**(7).

Liao, H. and J. H. Seinfeld (2005). "Global impacts of gas-phase chemistry-aerosol interactions on direct radiative forcing by anthropogenic aerosols and ozone." Journal of Geophysical Research-Atmospheres **110**(D18).

Martinez, M., D. Perner, et al. (2000). "NO_3 at Helgoland during the NORDEX campaign in October 1996." Journal of Geophysical Research-Atmospheres **105**(D18): 22685-22695.

Matsumoto, J., K. Imagawa, et al. (2006). "Nocturnal sink of NO_x via NO_3 and N_2O_5 in the outflow from a source area in Japan." Atmospheric Environment **40**(33): 6294-6302.

Mentel, T. F., M. Sohn, et al. (1999). "Nitrate effect in the heterogeneous hydrolysis of dinitrogen pentoxide on aqueous aerosols." Physical Chemistry Chemical Physics **1**(24): 5451-5457.

Murphy, J.G., Day, D.A., Cleary, P.A. , Wooldridge, P.J., Millet, D.B. , Goldstein, A.H., and Cohen, R.C. (2006a). "The weekend effect within and downwind of Sacramento: Part 1. Observations of ozone, nitrogen oxides, and VOC reactivity." Atmos. Chem. Phys. Disc. **6**: 11427-11464.

Murphy, J.G., Day, D.A., Cleary, P.A. , Wooldridge, P.J., Millet, D.B. , Goldstein, A.H., and Cohen, R.C. (2006b). "The weekend effect within and downwind of Sacramento: Part 2. Observational evidence for chemical and dynamical contributions." Atmos. Chem. Phys. Disc. **6**: 11971-12019.

Nelson, H. H., L. Pasternack, et al. (1983). "Laser-Induced Excitation and Emission-Spectra of NO_3." Journal of Physical Chemistry **87**(8): 1286-1288.

Orphal, J., C. E. Fellows, et al. (2003). "The visible absorption spectrum of NO_3 measured by high-resolution Fourier transform spectroscopy." Journal of Geophysical Research-Atmospheres **108**(D3).

Platt, U. and M. Hausmann (1994). "Spectroscopic Measurement of the Free-Radicals NO_3, BrO, IO, and OH in the Troposphere." Research on Chemical Intermediates **20**(3-5): 557-578.

Robinson, G. N., D. R. Worsnop, et al. (1997). "Heterogeneous uptake of $ClONO_2$ and N_2O_5 by sulfuric acid solutions." Journal of Geophysical Research-Atmospheres **102**(D3): 3583-3601.

Sander et al., NASA/JPL Data Evaluation, 2006

Sen, B., G. C. Toon, et al. (1998). "Measurements of reactive nitrogen in the stratosphere." Journal of Geophysical Research-Atmospheres **103**(D3): 3571-3585.

Simpson, W. R. (2003). "Continuous wave cavity ring-down spectroscopy applied to in situ detection of dinitrogen pentoxide (N_2O_5)." Review of Scientific Instruments **74**(7): 3442-3452.

Slusher, D. L., L. G. Huey, et al. (2004). "A thermal dissociation-chemical ionization mass spectrometry (TD-CIMS) technique for the simultaneous measurement of peroxyacyl nitrates and dinitrogen pentoxide." Journal of Geophysical Research-Atmospheres **109**(D19).

Sommariva, R., M. J. Pilling, et al. (2007). "Night-time radical chemistry during the NAMBLEX campaign." Atmospheric Chemistry and Physics **7**: 587-598.

Steinbacher, M., C. Zellweger, et al. (2007). "Nitrogen oxide measurements at rural sites in Switzerland: Bias of conventional measurement techniques." Journal of Geophysical Research-Atmospheres **112**(D11).

Stockwell, W. R., F. Kirchner, et al. (1997). "A new mechanism for regional atmospheric chemistry modeling." Journal Of Geophysical Research-Atmospheres **102**(D22): 25847-25879.

Stutz, J., B. Alicke, et al. (2004). "Vertical profiles of NO_3, N_2O_5, O_3, and NO_x in the nocturnal boundary layer: 1. Observations during the Texas Air Quality Study 2000 (vol 109, art no D12306, 2004)." Journal of Geophysical Research-Atmospheres **109**(D16).

Vaughan, S., C. E. Canosa-Mas, et al. (2006). "Kinetic studies of reactions of the nitrate radical (NO_3) with peroxy radicals (RO_2): an indirect source of OH at night?" Physical Chemistry Chemical Physics **8**(32): 3749-3760.

Venables, D. S., T. Gherman, et al. (2006). "High sensitivity in situ monitoring of NO_3 in an atmospheric simulation chamber using incoherent broadband cavity-enhanced absorption spectroscopy." Environmental Science & Technology **40**(21): 6758-6763.

Wahner, A., T. F. Mentel, et al. (1998). "Gas-phase reaction of N_2O_5 with water vapor: Importance of heterogeneous hydrolysis of N_2O_5 and surface desorption of HNO_3 in a large teflon chamber." Geophysical Research Letters **25**(12): 2169-2172.

Wayne, R. P., I. Barnes, et al. (1991). "The Nitrate Radical - Physics, Chemistry, and the Atmosphere." Atmospheric Environment Part a-General Topics **25**(1): 1-203.

Winer, A. M., J. W. Peters, et al. (1974). "Response of Commercial Chemiluminescent NO-NO_2 Analyzers To Other Nitrogen-Containing Compounds." Environmental Science & Technology **8**(13): 1118-1121.

Wood, E. C., P. J. Wooldridge, et al. (2003). "Prototype for in situ detection of atmospheric NO_3 and N_2O_5 via laser-induced fluorescence." Environmental Science & Technology **37**(24): 5732-5738.

Wood, E. C., T. H. Bertram, et al. (2005). "Measurements of N_2O_5, NO_2, and O_3 east of the San Francisco Bay." Atmospheric Chemistry and Physics **5**: 483-491.

Yokelson, R. J., J.B. Burkholder, R.W. Fox, R.K.Talukkdar, and A.R. Ravishankara (1994). "Temperature Dependence of the NO_3 Absorption Spectrum." Journal of Physical Chemistry **98**(50): 13144-13150.

Zador, J., T. Turanyi, et al. (2006). "Measurement and investigation of chamber radical sources in the European Photoreactor (EUPHORE)." Journal of Atmospheric Chemistry **55**(2): 147-166.

Zhou, D. K., G. E. Bingham, et al. (1997). "Stratospheric CH_4, N_2O, H_2O, NO_2, N_2O_5, and $ClONO_2$ profiles retrieved from cryogenic infrared radiance instrumentation for shuttle (CIRRIS 1A)/STS 39 measurements." Journal of Geophysical Research-Atmospheres **102**(D3): 3559-3573.